

Physical property and biological activity of bioscaffold containing the extracted native collagen and acemannan on proliferation and growth factor secretion in primary human pulpal cells



A Dissertation Submitted in Partial Fulfillment of the Requirements
for the Degree of Doctor of Philosophy in Dental Biomaterials Science

Inter-Department of Dental Biomaterials Science

GRADUATE SCHOOL

Chulalongkorn University

Academic Year 2021

Copyright of Chulalongkorn University

การศึกษาคุณสมบัติทางกายภาพและชีวภาพของโครงร่างชีววัสดุที่มีเนทีพคอลลลาเจนและอะซีแมนแนน
นต่อการเพิ่มจำนวนและการหลั่งโกรทแฟกเตอร์ ในเซลล์เนื้อเยื่อโครงฟัน



วิทยานิพนธ์นี้เป็นส่วนหนึ่งของการศึกษาตามหลักสูตรปริญญาวิทยาศาสตรดุษฎีบัณฑิต
สาขาวิชาทันตชีววัสดุศาสตร์ (สหสาขาวิชา) สหสาขาวิชาทันตชีววัสดุศาสตร์
บัณฑิตวิทยาลัย จุฬาลงกรณ์มหาวิทยาลัย
ปีการศึกษา 2564
ลิขสิทธิ์ของจุฬาลงกรณ์มหาวิทยาลัย

Thesis Title Physical property and biological activity of bioscaffold
 containing the extracted native collagen and acemannan on
 proliferation and growth factor secretion in primary human
 pulpal cells

By Miss Aye Aye Thant

Field of Study Dental Biomaterials Science

Thesis Advisor Professor Pasutha Thunyakitpisal

Accepted by the GRADUATE SCHOOL, Chulalongkorn University in Partial Fulfillment
of the Requirement for the Doctor of Philosophy

..... Dean of the GRADUATE SCHOOL
(Associate Professor YOOTTHANA CHUPPUNNARAT)

DISSERTATION COMMITTEE

..... Chairman
(Professor Sittichai Koontongkaew)

..... Thesis Advisor
(Professor Pasutha Thunyakitpisal)

..... Examiner
(Associate Professor PAIROJ LINSUWANONT)

..... Examiner
(Associate Professor WANPEN TACHABOONYAKIAT)

..... Examiner
(Associate Professor WIJIT BANLUNARA)

..... Examiner
(Associate Professor VIRITPON SRIMANEEPONG)

เอย์ เอย์ ธานท์ :

การศึกษาคุณสมบัติทางกายภาพและชีวภาพของโครงร่างชีววัสดุที่มีเนทีพอลลาเจนและอะซีแมนแนนต่อการเพิ่มจำนวนและการหลั่งโกรทแฟกเตอร์ ในเซลล์เนื้อเยื่อโพรงฟัน. (Physical property and biological activity of bioscaffold containing the extracted native collagen and acemannan on proliferation and growth factor secretion in primary human pulpal cells) อ.ที่ปรึกษาหลัก : พสุธา ธีัญญะกิจไพศาล

การสร้างเนื้อเยื่อโพรงฟันเป็นแนวความคิดที่อาศัยองค์ความรู้ด้านวิศวกรรมเนื้อเยื่อซึ่งประกอบด้วย สเต็ ม เ ซ ล ล ์ โ ค ร ง ร ำ ง และโกรทแฟกเตอร์ โดยสารสกัดคอลลาเจนจากสัตว์นิยใช้เป็นโครงร่างเนื่องจากมีความเข้ากันกับเนื้อเยื่อและสลายตัวได้ในร่างกาย รวมทั้งมีคุณสมบัติที่คล้ายคลึงกับสารเมทริกซ์นอกเซลล์ในร่างกาย อย่างไรก็ตามบทบาทของสารสกัดคอลลาเจนในแง่การเพิ่มจำนวน การเปลี่ยนสภาพและการสร้างเนื้อเยื่อใหม่ที่จำเป็นต่อการสร้างเนื้อเยื่อโพรงฟันเพื่อการเติบโตของฟันและรากยังไม่เป็นที่แน่ชัด นักวิทยาศาสตร์ได้เสนอแนะการเติมสารชีวโมเลกุลลงในโครงร่างคอลลาเจนเพื่อช่วยในการสร้างเนื้อเยื่อโพรงฟัน อะซีแมนแนนเป็น พ อ ลี แ ซ ค ค า ไ ร ต์ พ อ ลี แ ม น น อ ส ส กั ต จ า ก ว่า น ท า ง จ ร ะ เ ซ้ อะซีแมนแนนมีบทบาทเป็นชีวโมเลกุลเพื่อสร้างเนื้อเยื่อใหม่และควบคุมการตอบสนองของภูมิคุ้มกัน ในการศึกษาครั้งนี้สารอะซีแมนแนนและคอลลาเจนสกัดจากว่านหางจระเข้และผิวหนังกุ้งสกัดด้วยเทคนิคสกัดเย็นและพิสูจน์เอกลักษณ์ พัฒนาโครงร่างคอลลาเจน-อะซีแมนแนนด้วยเทคนิคการทำแห้งแบบแช่เยือกแข็ง ทดสอบคุณสมบัติทางกายภาพด้วยเทคนิคเอฟทีไออาร์ กล้องจุลทรรศน์อิเล็กตรอนแบบส่องกราด มุมสัมผัส การบวมน้ำและการสลายตัว รวมทั้งทดสอบความเข้ากันได้กับเซลล์ ผลต่อการหลั่งโกรทแฟกเตอร์ โปรตีนที่เกี่ยวข้องกับการสร้างกระดูกและการตกตะกอนแร่ธาตุในระดับห้องปฏิบัติการ ผลการศึกษานี้ พบว่า โครงร่างอะซีแมนแนน-คอลลาเจนมีความชอบน้ำและการบวมน้ำที่ดีกว่าโครงร่างคอลลาเจนอย่างมีนัยสำคัญทางสถิติ ($p < 0.05$) โครงร่างอะซีแมนแนน-คอลลาเจนกระตุ้นการแบ่งตัวเพิ่มจำนวน การสร้างโกรทแฟกเตอร์ วิอีจีเอฟ และ บีเอ็มพี -2 เมื่อเทียบกับโครงร่างคอลลาเจนอย่างมีนัยสำคัญทางสถิติ ($p < 0.05$) มีการยึดเกาะที่ดีระหว่างเซลล์และเซลล์กับโครงร่าง พบการแสดงออกของโปรตีนออสทีโอพอนทินและโบนไซอะโลพอสโฟโปรตีนในโครงร่างทั้งสองแบบ ยกเว้นโปรตีนเดนทินไซอะโลพอสโฟโปรตีนที่พบเฉพาะในโครงร่างอะซีแมนแนน-คอลลาเจนเท่านั้น จากการศึกษาครั้งนี้สรุปได้ว่า โครงร่างอะซีแมนแนน-คอลลาเจนให้ผลเสริมฤทธิ์กันทั้งในด้านกายภาพและชีวภาพที่ดีกว่าโครงร่างคอลลาเจน ดังนั้นโครงร่างอะซีแมนแนน-คอลลาเจนจึงเหมาะต่อการใช้ในการสร้างเนื้อเยื่อโพรงฟัน

สาขาวิชา ทันตชีววัสดุศาสตร์ (สหสาขาวิชา)

ลายมือชื่อนิสิต

ปีการศึกษา 2564

ลายมือชื่อ อ.ที่ปรึกษาหลัก

6187837120 : MAJOR DENTAL BIOMATERIALS SCIENCE

KEYWORD: Acemannan, Collagen, Scaffolds, Tissue regeneration

Aye Aye Thant : Physical property and biological activity of bioscaffold containing the extracted native collagen and acemannan on proliferation and growth factor secretion in primary human pulpal cells. Advisor: Prof. Pasutha Thunyakitpisal

Dental pulp tissue regeneration is based on tissue engineering concepts using stem cells, scaffolds, and growth factors to regenerate the pulp-dentine complex. Up to now, native collagen is commonly used as a biomaterial scaffold for tissue regeneration due to its biocompatibility, biodegradability, and properties that mimic the natural extracellular matrix (ECM). However, the bioactivity of collagen scaffold on cell growth and differentiation, and regenerative activities such as extracellular matrix formation and growth factor secretion which are important for pulp revascularization and regeneration and accomplishment root formation is still unclear. Many studies elucidated that adding biomolecules into the collagen scaffold enhanced pulp regeneration. Acemannan, β -(1-4)-acetylated polymannose, is a major polysaccharide extracted from aloe vera. Acemannan functions as an immunomodulator and regenerative biomaterial. Therefore, acemannan could be alternative biomolecule for collagen scaffold. In this study, acemannan and native collagen were cold extracted from aloe vera and porcine skin, respectively, and characterized. The acemannan-collagen (AceCol) scaffolds were prepared using freeze-drying method. The physical properties of AceCol scaffold were investigated using FTIR, SEM, contact angle, swelling, and degradation tests. *In vitro*, biocompatibility, growth factor secretion, osteogenic proteins expression, and mineral deposition were also evaluated. Our results revealed that the AceCol scaffold has higher hydrophilicity and swelling properties rather than that of collagen scaffold ($p < 0.05$). Better cell-cell and cell-scaffold adhesions, and dentin extracellular matrix (BSP, OPN, and DSPP) expression were observed in the AceCol scaffold. Only AceCol group show DSPP expression, while the collagen group did not. Significant increasing of cellular proliferation, VEGF and BMP2 expression, and mineral deposition was detected in the AceCol scaffold compared with that of collagen scaffold ($p < 0.05$). In conclusion, the AceCol scaffold has synergistically provided the better physical and biological properties rather than each individual part. AceCol scaffold is a promising material for tissue regeneration.

Field of Study: Dental Biomaterials Science

Student's Signature

Academic Year: 2021

Advisor's Signature

ACKNOWLEDGEMENTS

First of all, I would like to express my sincere thanks and gratitude to my thesis advisor Professor Pasutha Thunyakitipisal for his continuous guidance, support, and encouragement throughout my Ph.D journey. My thesis would not have been accomplished without the guidance and support that I have ever received from him. I would like to thank Associate Professor Wijit Banlunara and Dr. Benchaphorn Limcharoen for their kind guidance, support, and valuable suggestions for my research work.

I would like to thank my thesis committee, Professor Sittichai Koontongkaew, Associate Professor Pairoj Linsuwanont, Associate Professor Wijit Banlunara, Assistant Professor Wanpen Tachaboonyakiat, and Associate Professor Viritpon Srimeaneepong for giving their valuable time, suggestions, comments, and sharing their ideas for improving my dissertation.

Thank you to all my colleagues in the Dental Biomaterials Science Program for their help, supports, and cooperation throughout my project.

In addition, I would like to acknowledge 100th year anniversary Chulalongkorn University Scholarship committee for giving me a chance to study Ph.D. degree at Chulalongkorn University.

Finally, I am grateful to my family and all my friends for their support. I would not have accomplished my Ph.D. study without their support, love, and encouragement. I thank all who are not mentioned but provided support and help in the completion of my Ph.D. study. I would not come so far like this without them.

Aye Aye Thant

TABLE OF CONTENTS

	Page
ABSTRACT (THAI).....	iii
ABSTRACT (ENGLISH).....	iv
ACKNOWLEDGEMENTS.....	v
TABLE OF CONTENTS.....	vi
LIST OF TABLES.....	x
LIST OF FIGURES.....	xi
Chapter I.....	1
Introduction.....	1
1.1 Background and rationale.....	1
1.2 Research question.....	3
1.3 Research hypothesis.....	3
1.5 Conceptual framework.....	4
Chapter 2.....	5
Literature review.....	5
2.1 Tissue engineering concepts in dentistry.....	5
2.1.1 Sources of stem cells in pulp tissue regeneration.....	5
2.1.2 Role of growth factors in pulp tissue regeneration.....	6
2.1.3 Scaffolds in pulp tissue regeneration.....	7
2.2 Collagen in dentistry.....	8
2.2.1 Structure of the collagen.....	8
2.2.2 Types of collagen.....	9

2.2.3. Sources of collagen extraction	11
2.2.4. Collagen extraction methods	11
2.2.5. Uses of collagen scaffold in dental tissue regeneration	12
2.3 Acemannan, an extracted polysaccharide from <i>Aloe vera</i>	13
2.3.1 Aloe vera	13
2.3.2 Active ingredients.....	14
2.3.3 Acemannan	14
2.3.4 Isolation and characterization of Acemannan	15
2.3.5 Acemannan in dentistry	15
2.3.6 Role of acemannan in pulp tissue regeneration	17
Chapter III	18
Materials and methods.....	18
Part I. Collagen extraction and characterization.....	18
1.1 Extraction of collagen from porcine skin	18
1.2 Characterization of the extracted porcine collagen	18
1.2.1 Total amino acid analysis.....	18
1.2.2 SDS-PAGE analysis.....	19
1.2.3 Western blot analysis.....	19
1.2.4 CD spectrophotometer.....	20
Part II. Extraction and characterization of acemannan.....	20
Part III. AceCOL scaffold preparation.....	20
Part IV. Physical characterization of AceCol scaffold	21
4.1 Morphological analysis.....	21
4.2 Contact angle measurement	21

4.3 Swelling test.....	21
4.4 Degradation test.....	22
4.5 Fourier-transform infrared spectroscopy (FTIR) analysis.....	22
Part V. In vitro biocompatibility and biological activity of AceCol scaffolds	22
5.1 Cell culture.....	22
5.2 MTT and ELISA.....	22
5.3 SEM	23
5.4 Immunofluorescence evaluation.....	23
5.5 Calcium concentration measurement.....	24
5.6 Computational simulations.....	24
Statistical Analysis.....	26
Chapter IV.....	27
Results.....	27
4.1 Porcine skin collagen extraction and characterization.....	27
4.2 Characterization of the AceCol scaffolds	28
4.3 Morphology analysis with SEM.....	30
4.4 Biocompatibility and growth factors secretion of collagen and AceCol scaffolds	31
4.5 Cell adhesion and extracellular matrix formation	33
4.6 Immunofluorescence evaluation of osteogenic proteins expression	35
4.7 Mineral deposition	35
4.8 Computational simulation.....	36
Chapter V.....	39
Discussion.....	39

Chapter VI.....	43
Conclusion	43
REFERENCES	44
VITA.....	56



LIST OF TABLES

	Page
Table 1 Role of growth factors in pulp regeneration adapted from Piva, et al. (2014)[24].....	6
Table 2 The various collagen types and their distribution Photo curtesy from Gelse et al (2003) [36].....	9
Table 3 Use of collagen scaffold in pulp regeneration.....	13
Table 4 active ingredients of Aloe vera leaf.....	14
Table 5 Summary various studies of acemannan	15
Table 6 Bioactivity of acemannan in dentistry.....	16
Table 7 Composition and abbreviations of scaffolds.....	21
Table 8 Percentage amino acid composition of the extracted porcine skin collagen.	27
Table 9 Nine modes of the highest binding energies of single strand acemannan model: β -(1,4)-acetylated polymannose with β -(1,4) glucose and α -(1,6)-linked galactose side-chain (SAC1) and 1,4 glycosidic linkage of acetylated polymannose (SAC2) dock against collagen molecule (COL).....	36

LIST OF FIGURES

	Page
Figure 1 Sources of stem cells. Photo courtesy from Manivasagam, et al. (2019)[21].	6
Figure 2 a collagen triple helix (cross-sectional). G-glycine, X- proline, and Y-hydroxyproline. Photo courtesy from Hulmes, 2008[32].	8
Figure 3 Schematic presentation of the type I collagen quaternary structure. (D = 67nm)	9
Figure 4 Schematic presentation of the position of N- and C- terminal antigenic P-determinant sequence of telopeptide region for pepsin digestion. Photo courtesy from Lynn, et al. (2004) [49].	12
Figure 5 Structure of the mucopolysaccharide acemannan, extracted from Aloe vera. It is Beta-(1,4)-acetylated polymannose.	14
Figure 6 Molecule of acemannan (a) SAC1 and (b) SAC2 model. Top, middle, and bottom images are structural formula, AM1-optimized structures, and the highest binding affinity form to bind collagen which based on molecular docking algorithm, respectively. (c) molecular structure of the collagen type I (COL) with hydrophobicity surface. The COL was taken from the PDB [109]. The graphic was visualized by the program UCSF Chimera [110].	25
Figure 7 The extracted collagen was characterized using (a) immunoblot analysis of 2 and 5 mg of the protein (b) Circular dichroism (CD) spectroscopy of the extracted collagen. The negative and positive bands are detected at 197 and 222 nm, respectively.	28
Figure 8 FTIR analysis of the representative collagen and acemannan-collagen scaffolds demonstrated the peak of carbonyl group of acemannan (1740), amide groups of collagen (1679 and 1542).	29

Figure 9 The representative collagen and acemannan-collagen scaffolds (a) Water contact angle measurement, (b) Swelling ratio, and (c) degradation rate. N=4. * Statistically significant difference from collagen, ($p < 0.05$).	30
Figure 10 SEM images of scaffold morphology; collagen, AceCol 1, AceCol 2, and AceCol 3 scaffolds.	31
Figure 11 Cell viability at 24 h. Dental pulp cells were treated with the condition media of Col, AceCol1, AceCol2, and AceCol3., *, # Statistically significant difference from control and collagen groups, respectively ($p < 0.05$).	31
Figure 12 Dental pulp cells were treated with the condition media of Col, AceCol1, AceCol2, and AceCol3. (a) BMP2 at 72 h, and (b) VEGF expression at 24 h. *, # Statistically significant difference from control and collagen groups, respectively ($p < 0.05$).	32
Figure 13 SEM images of human dental pulp cells attachment and the scaffold morphology at 4 h, 3 days, 7 days, and 14 days post-incubation on Col and AceCol1 scaffolds. Cells were seeded on the scaffold and cultured in growth culture media. The fresh media was replaced every couple day.	33
Figure 14 DAPI staining of the nucleus of the cells distributed over the scaffolds at 1 day, 3 days, 7 days, and 14 days post-incubation. Cells were seeded on the scaffold and cultured in growth culture media. The fresh media was replaced every couple day.	34
Figure 15 Osteogenic protein expressions were evaluated using immunofluorescence staining technique. Cells were seeded in Col and AceCol scaffolds and incubated for 3 days. (a) Bone sialoprotein (BSP) stained with Alexa fluor 488, (b) Osteopontin (OP) stained with Alexa fluor 647, and (c) Dentin Sialophosphoprotein (DSPP) stained with Alexa fluor 568. Cellular nuclei were counterstained with DAPI. Magnification x10. Insert image magnification x100.	35
Figure 16 Graphical representation of (a) SAC1-COL complex based on the highest affinity of SAC1 binding to COL (b) SAC1-(SAC1-COL) complex obtained from the highest affinity of secondary SAC1 molecule binding to SAC1-COL complex. The	

binding energies of first and second SAC1 onto the COL and the SAC1-COL are -3.9 and -4.2 kcal/mol, respectively. 37

Figure 17 Graphical representation of (a) SAC2-COL complex obtained from the highest affinity of SAC2 binding to COL (b) SAC2-(SAC2-COL) complex based on the highest affinity of secondary SAC2 molecule binding to SAC2-COL complex. The binding energies of first and second SAC2 onto the COL and the SAC2-COL are -3.6 and -3.3 kcal/mol, respectively. 38



Chapter I

Introduction

1.1 Background and rationale

Up to now, the regenerative endodontic approach has been introduced to overcome the drawbacks of the earlier apexification treatment in the case of immature permanent teeth with necrotic pulp. This new approach is based on the combination of endogenous stem cells obtained from an intentional induced bleeding and blood clot scaffolds [1]. Natural and synthetic biomaterials are suggested as alternative materials because provoked bleeding can be a compromised situation for both clinicians and patients. The accomplishment of an ideal scaffold for pulp regeneration becomes a critical procedure. The scaffold should have the native extracellular matrix (ECM) characteristic, providing a three-dimensional matrix for cell migration and proliferation and a suitable regeneration environment for new tissue formation. Now, native collagen is commonly used as a natural scaffold for tissue regeneration owing to its biocompatibility, biodegradability, and properties that mimic the natural ECM [2, 3]. Moreover, collagen is the main extracellular matrix component of the pulp tissue, so it is an excellent dental pulp tissue regeneration platform. Many studies elucidated that adding biomolecules such as BMP-2, VEGF, PDGF, and bFGF into the collagen scaffold improved dental pulp tissue regeneration [4, 5].

Likewise, acemannan, β -(1-4)-acetylated polymannose, is a major polysaccharide extracted from aloe vera. Acemannan functions as an immunomodulator and regenerative biomaterial [6, 7]. With unique acetylated mannose molecules, this polysaccharide induces cell proliferation, growth factor and extracellular matrix synthesis, and mineral deposition [8]. In animal and clinical studies, used as capping material for direct pulp exposure and partial pulpotomy, acemannan enhances reparative dentin formation in primary and immature permanent teeth. Radiography and histological analysis demonstrated healthy

remaining pulp tissue, osteodentin bridge-covered exposure area, and continued root formation[8-10]. Therefore, acemannan could be the alternative biomolecule to enhance the properties of collagen scaffold.

In the present study, acemannan and native collagen were cold extracted from aloe vera gel and porcine skin, respectively. Acemannan-Collagen bioscaffold has been developed using homogenizing and freeze-drying methods. The resulting scaffold was characterized by SEM, contact angle, swelling and degradation tests, and FTIR. *In vitro* biocompatibility, bioactivity, osteogenic proteins expression, and calcification were also analyzed.



1.2 Research question

Does the combination of acemannan and collagen to generate bioscaffold synergize the advantages of both materials?

1.3 Research hypothesis

Hypothesis 1.

Independent variables: Collagen scaffold, AceCOL scaffolds

Dependent variables: physical property; contact angle measurement, swelling and degradation, FTIR, SEM

H0: There was no significantly different effect between the collagen scaffold and AceCol scaffold on the physical properties such as contact angle measurement, swelling and degradation, FTIR, SEM.

H1: There was significantly different effect between the collagen scaffold and AceCol scaffold on the physical properties such as contact angle measurement, swelling and degradation, FTIR, SEM.

Hypothesis 2.

Independent variables: Collagen scaffold, AceCOL scaffolds

Dependent variables: biological property; Cell toxicity, growth factor secretion, osteogenic protein expression, mineral deposition

H0: There was no significantly different effect between the collagen scaffold and AceCol scaffold on the biological properties such as Cell toxicity, growth factor secretion, osteogenic protein expression, mineral deposition.

H1: There was significantly different effect between the collagen scaffold and AceCol scaffold on the biological properties such as Cell toxicity, growth factor secretion, osteogenic protein expression, mineral deposition.

1.4 Objectives of the study

Objective 1: To extract and characterize the native collagen from porcine skin

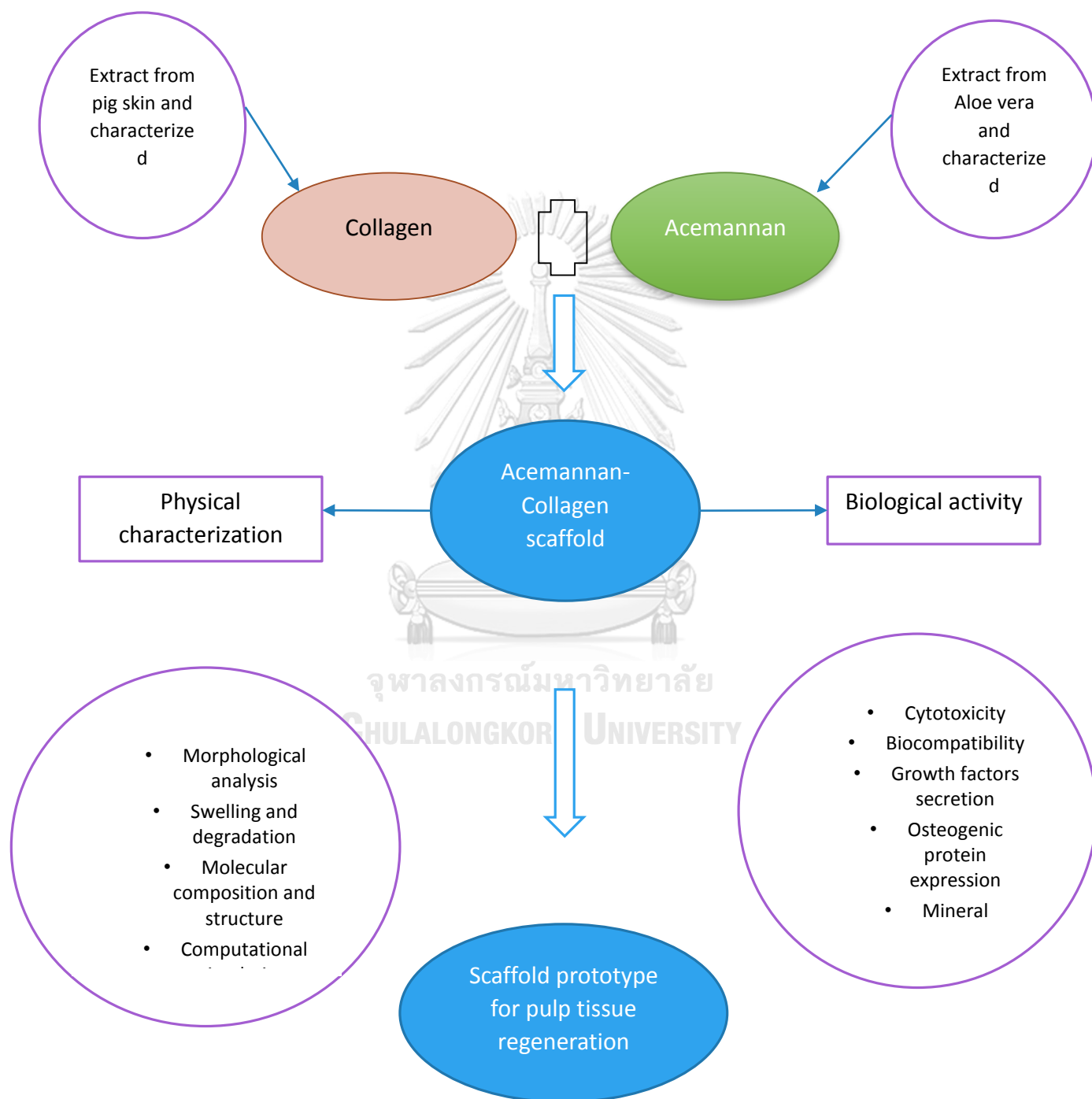
Objective 2: To extract and characterize acemannan from aloe vera

Objective 3: To prepare AceCol scaffolds

Objective 4: To investigate the physical properties of AceCol scaffolds

Objective 5: To investigate the biocompatibility and biological activities of AceCol scaffolds in human dental pulp cell

1.5 Conceptual framework



Chapter 2

Literature review

2.1 Tissue engineering concepts in dentistry

Root canal therapy has been the standard endodontic treatment for teeth with irreversibly damaged pulp[11]. Even though positive results are observed following endodontic treatment, downsides are a weakened tooth with significant loss of tooth structure and loss of vitality[11]. In developing permanent dentition, the trauma, caries, or developmental anomalies such as dens invaginatus can cause pulp necrosis and periapical periodontitis. Loss of tooth vitality in these teeth affects tooth development and subsequent interruption of the root formation, leading to thin root walls and open root apex[12],[13]. To overcome these problems and maintain tooth vitality, dental tissue regeneration - the natural replacement of injured tooth structures - is the alternative to pulp capping and root canal treatment. Pulp tissue regeneration strategies are based on tissue engineering concepts in which damaged pulp is partially or entirely removed and replaced with healthy pulp instead of conventional root canal therapy[14].

Pulp-dentine complex regeneration is based on three elements - stem cells, scaffolds, and growth factors. There are two approaches to pulp regeneration, cell-based and cell-free regeneration. Cell-based pulp regeneration utilized the mesenchymal stem cells (MSC) from dental pulp, natural or synthetic scaffolds, and growth factors. Nevertheless, isolation, storage, and implantation of MSC is still a big challenge[15]. As an alternative option, the cell-free pulp regeneration approach employed the bioactive scaffolds and growth factors to attract the endogenous pulp stem cells from the remaining pulp or apical papilla into the endodontic space[16-18].

2.1.1 Sources of stem cells in pulp tissue regeneration

The stem cells from apical papilla (SCAP) are suggested to be the primary stem cell source in cell-free regenerative endodontic in immature permanent teeth because of their proximity to the root apex[19]. There is evidence that the stem cells

from apical papilla can differentiate into odontoblast-like cells and produce dentine in the root canal[20]. Dental pulp stem cells (DPSCs) can differentiate into odontoblast based on growth factors and signaling molecules activities[21]. Therefore, DPSCs can be used to restore injured pulp tissues. Other stem cells that can be used are stem cells of human exfoliated deciduous teeth (SHED) and periodontal ligament cells (PDLSCs) (fig 1.)

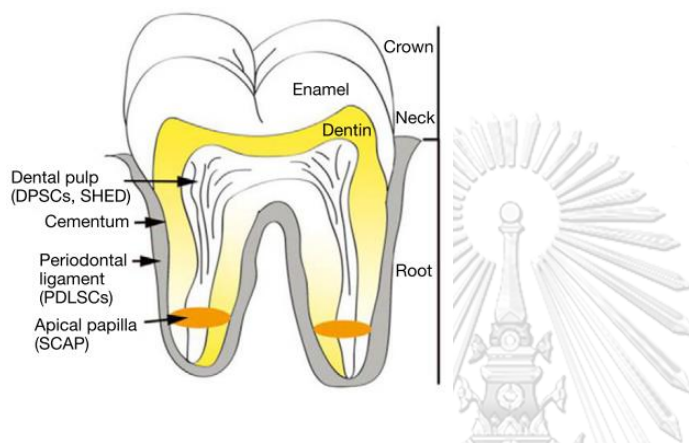


Figure 1 Sources of stem cells. Photo courtesy from Manivasagam, et al. (2019)[21].

2.1.2 Role of growth factors in pulp tissue regeneration

Vasculature in the pulp tissue plays a critical role in nutrition and oxygen supply, functions as a tool for the transport of metabolic waste, nutrients, growth factors, and regulates inflammation. For pulp tissue regeneration, growth factors play a role in regulating vasculature renewal and proliferation and odontoblast differentiation. Platelet derived growth factor (PDGF) and vascular endothelial growth factor (VEGF) increased renewal of vasculature in an early phase of healing and increased their proliferation. Bone morphogenetic protein 2 (BMP-2) regulates odontogenic differentiation of DPSC and SCAP and stimulates mineralization of newly formed matrix essential for the dentin-pulp complex regeneration. It also acts synergistically with VEGF for pulp regeneration[22]. Fortunately, these growth factors are entombed in the extracellular matrix of dentine and can thus be released or exposed by the conditioning of the dentine surface[23].

Table 1 Role of growth factors in pulp regeneration adapted from Piva, et al. (2014)[24]

Protein	Potential role in dental pulp regeneration
Bone morphogenetic protein 2, 7	SHED differentiation into dental pulp cells mineralized tissue formation on dental pulp stem cells <i>in vitro</i> and <i>in vivo</i>
Fibroblast growth factor-2	Cell proliferation and revascularization of human teeth inserted into the rat dorsum and stimulates the dental tissue mineralization
Transforming growth factor beta 1	Odontoblast-like cell differentiation and DPSC-mediated mineralization <i>in vitro</i>
Vascular endothelial growth factor	Endothelial cell formation by SHED differentiation

DPSc- dental pulp stem cells, HDPC- human dental pulp cell, SHED-stem cells from exfoliated deciduous teeth.

2.1.3 Scaffolds in pulp tissue regeneration

A variety of biomaterials is available as a scaffold can be divided into biopolymers, metals, ceramics, and composite materials that mix any two different classes of materials (fig.2). The metals and ceramics are mainly used in bone and cartilage regeneration while biopolymers are used in soft tissue regeneration. Each material presents unique chemistry, structure, composition, and degradation properties. The role of the scaffold has improved from passive carrier toward a bioactive matrix, which can induce a desired cellular behavior[25].

Blood clot is created by intentional bleeding through periapex with sharp instrument and used as scaffold and also source of growth factors[26]. However, provoking the bleeding into root canal space is not always achievable[27], and the nature of the blood clot is unstable[28]. Thus, the natural and synthetic polymers are suggested to use as scaffolds being a more predictable alternative for regenerative endodontics and pulp tissue regeneration[29]. Natural polymers are

derived from renewable resources, plants, animals, and microorganisms, and they are widely distributed in nature, for example, collagen, chitosan, and chitin.

2.2 Collagen in dentistry

2.2.1 Structure of the collagen

Collagen is a fibrous protein found abundantly in all multicellular animals [30] and important in functions to support organs such as bones, skin, muscles, tendons, and ligaments. It is related to approximately 25% weight of all proteins in the body [31].

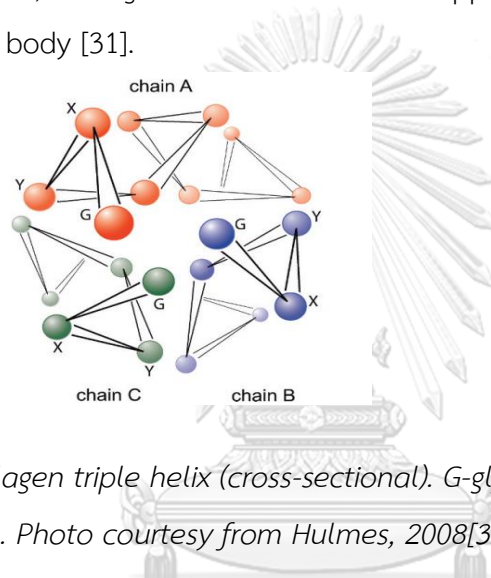


Figure 2 a collagen triple helix (cross-sectional). G-glycine, X- proline, and Y-hydroxyproline. Photo courtesy from Hulmes, 2008[32].

The primary feature of the collagen is helix with three alpha chains [33, 34]. These three chains are coiled around a central axis in a right-handed manner to form a triple helix [33]. Glycine, the smallest amino acid, occurs in every third position of the polypeptide chain to create (Gly-X-Y), typical collagen repeats. The alpha chains assemble around a central axis that all glycine residues are in the center of the triple helix. The side chains of other amino acids are outer positions. X and Y position is mainly proline and hydroxyproline and Gly-X-Y is the most common form (fig. 3). Proline and hydroxyproline represent about 23% of the total protein structure [35]. According to the different types, collagen has three identical chains (homotrimers) and different chains (heterotrimers). For example, type I collagen molecule is heterotrimer. Two of the alpha chains are identical and the third is distinct, written as $[\alpha 1(I)]_2 \alpha 2$. In type II collagen, the triple helix comprises three $\alpha 1(II)$ -chains forming a

homotrimeric molecule. Type III collagen is a homotrimer of three $\alpha 1$ (III)-chains. Six subunit chains of type IV collagen have been identified yet, $\alpha 1$ (IV) – $\alpha 6$ (IV), associating into three distinct heterotrimeric molecules. The predominant form is represented by $\alpha 1$ (IV)₂ $\alpha 2$ (IV) heterotrimers [36].

Fibril forming collagen usually forms fibrils with a length of 300 nm and a fibrillary diameter of up to 1000 nm. Molecules of collagen are parallel and overlap each other. Each distance between overlap is 67 nm (distance D), with length of each molecule is 4.4 D (300 nm). There is a 40-nm (0.6 D) gap between adjacent molecules to form quarter-staggered assembly (Fig. 4).

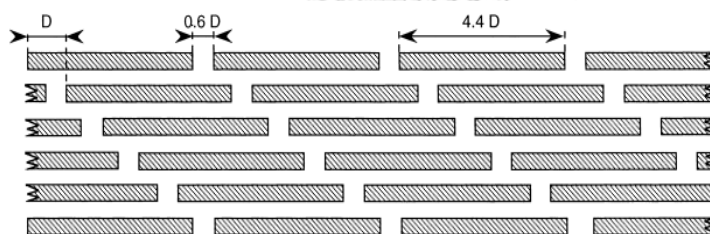


Figure 3 Schematic presentation of the type I collagen quaternary structure. ($D = 67\text{nm}$)

(Photo courtesy from Rossert and Crombrughe (2002) [37])

2.2.2 Types of collagen

So far, twenty-eight types of collagen have been discovered and characterized. Collagens can be grouped into several subfamilies based on their structure and supramolecular organization: fibril forming collagens (type I, II, III, V and XI), fibril-associated collagens with interrupted triple helix (FACIT) (type IX, XII, and XIV), network-forming collagens (type VIII, X), anchoring fibrils (type VII), transmembrane collagens (type XIII, XVII), basement membrane collagen (type IV), and others with unique functions [36].

Table 2 The various collagen types and their distribution Photo curtesy from Gelse et al (2003) [36].

Types of collagen	Tissue distribution
Fibril-forming collagens	
I [$\alpha 1$ (I)] ₂ $\alpha 2$ (I)	Bone, dermis, tendon, ligaments, cornea
II [$\alpha 1$ (II)] ₃	Cartilage, vitreous body, nucleus pulposus
	Skin, vessel wall, reticular fibres of most tissues

III [$\alpha 1$ (II)] ₃	(lungs, liver, spleen, etc.)
V $\alpha 1$ (V), $\alpha 2$ (V), $\alpha 3$ (V)	Lung, cornea, bone, fetal membranes; together with type I collagen Cartilage, vitreous body
XI $\alpha 1$ (XI) $\alpha 2$ (XI) $\alpha 3$ (XI) Basement membrane collagens	Basement membranes
IV [$\alpha 1$ (IV)] ₂ $\alpha 2$ (IV); $\alpha 1 - \alpha 6$ Microfibrillar collagen	Widespread: dermis, cartilage, placenta, lungs, vessel wall, intervertebral disc
VI $\alpha 1$ (VI), $\alpha 2$ (VI), $\alpha 3$ (VI) Anchoring fibrils	Skin, dermal – epidermal junctions; oral mucosa, cervix
VII [$\alpha 1$ (VII)] ₃	
Hexagonal network-forming collagens	Endothelial cells, descemet's membrane
VIII [$\alpha 1$ (VIII)] ₂ $\alpha 2$ (VIII)	Hypertrophic cartilage
X [$\alpha 3$ (X)] ₃ FACIT collagens	Cartilage, vitreous humor, cornea
IX $\alpha 1$ (IX) $\alpha 2$ (IX) $\alpha 3$ (IX)	Perichondrium, ligaments, tendon
XII [$\alpha 1$ (XII)] ₃	Dermis, tendon, vessel wall, placenta, lungs, liver
XIV [$\alpha 1$ (XIV)] ₃	Human rhabdomyosarcoma
XIX [$\alpha 1$ (XIX)] ₃	Corneal epithelium, embryonic skin, sternal cartilage, tendon
XX [$\alpha 1$ (XX)] ₃	Blood vessel wall
XXI [$\alpha 1$ (XXI)] ₃ Transmembrane collagens	Epidermis, hair follicle, endomysium, intestine, chondrocytes, lungs, liver
XIII [$\alpha 1$ (XIII)] ₃	Dermal – epidermal junctions
XVII [$\alpha 1$ (XVII)] ₃ Multiplexins	Fibroblasts, smooth muscle cells, kidney, pancreas
XV [$\alpha 1$ (XV)] ₃	Fibroblasts, amnion, keratinocytes lungs, liver
XVI [$\alpha 1$ (XVI)] ₃	

2.2.3. Sources of collagen extraction

According to Yang and Shu (2014), there are two categories for collagen sources: the extracted collagen from natural sources and the synthesized collagen [38]. Many studies have been described that collagen can be successfully extracted from animal sources: skin, tendon, cartilage, and pericardium of mammals (primarily bovine and porcine in origin) [39, 40], marine sources [41, 42], and poultry (11). Nonetheless, significant collagen sources for biomedical applications include bovine skin, tendons, porcine skin, and rat tail. However, the bovine product has a risk of bovine spongiform encephalopathy [43] and poultry has a risk of transmitting avian influenza [44]. Major drawback of the marine collagen is low thermal resistance because of its low hydroxyproline content [45].

Because of the homology between porcine and human beings, porcine collagen is low antigenicity. Moreover, as a by-product of pork production, porcine skin can be easily obtained from the local markets. Thus, we use the porcine skin as the source for collagen extraction in this study.

2.2.4. Collagen extraction methods

Collagen can be extracted using a neutral salt solution method, acidic solution method, and combined acidic solution and proteolytic enzymes (pepsin, papain, trypsin, etc.) method [46]. The major barrier to the dissolution of collagen from tissue is the presence of intermolecular covalent crosslinks. The pattern of crosslinks determines the solvent to use and the corresponding yields. The 0.5M acetic acid is widely used for acidic extraction [47]. Acids cut only intermolecular aldimine cross-links so that the collagen extraction yield is lower than the combined method which cleaves more stable and mature ketoimine cross-links [48]. Pepsin is the most used enzyme for the combined method because this enzyme selectively removes the antigenic P-determinant sequence located at the telopeptide regions providing a better quality of extracted collagen [47]. For that reason, we use the

combined acidic solution and pepsin method in this study to extract porcine collagen.

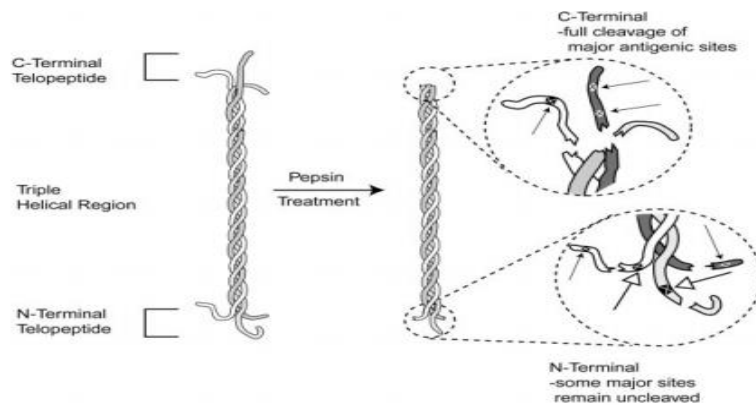


Figure 4 Schematic presentation of the position of N- and C- terminal antigenic P-determinant sequence of telopeptide region for pepsin digestion. Photo courtesy from Lynn, et al. (2004) [49].

2.2.5. Uses of collagen scaffold in dental tissue regeneration

Collagen is the extracellular matrix protein of the pulp and dentine matrix. Due to its 3D structure conformation, biocompatibility and biodegradability, native collagen is the most commonly used as a resorbable scaffold[2]. Besides, collagen enhances cell adhesion and survival[50]. Collagen has wide applications in dentistry, and it could be used as a membrane, bone graft, local drug delivery agent, and a hemostatic agent. For example, collagen plugs are being used to control oozing or bleeding from wounds, graft closure, and extraction socket to encourage healing [51]. Collagen membranes have been used for guided tissue regeneration (GTR) in periodontal reconstruction because it prevent epithelial migration provide haemostasis[52]. Collagen can also be used in plastic and reconstructive surgery as an graft in palatoplasty[53] and guided bone regeneration [54], bone augmentation for dental implants[55] and as a reconstructive material for maxillofacial fractures[56].

Collagen is appropriate as a scaffold material for pulp dentin regeneration. Various studies have elucidated *in vitro* and *in vivo* that collagen as sponge and gel scaffolds enhance proliferation of DPSCs and odontoblast differentiation[57-59]. Moreover, collagen has been used as a scaffold, stem cells, and growth factor (dentin matrix protein 1) to generate dental pulp-liked tissue *in vivo*[60]. Clinically,

collagen can also be used in regenerative endodontics. Jiang, et al. (2017) studied the effectiveness of collagen membrane as a scaffold and discovered that collagen promoted dentin formation in the middle third of the root wall in patients treating with regenerative endodontic procedures[61]. Collagen is synergic with the other bioactive components[62]. The combination of collagen with other polymers can enhance the physical, chemical, and biological properties of collagen [63-65].

Table 3 Use of collagen scaffold in pulp regeneration.

Materials	Method	Cell type	Finding	Reference
Collagen with BMP-2 and 4 & TGF- β 1	<i>In vivo</i>	Dog pulp cells	induce osteodentin formation	Nakashima, 1994[66]
Collagen with Ceramic powder & DMP-1	<i>In vivo</i>	DPSCs human	New pulp-like tissue formation	Prescott, et al. (2008) [60]
Collagen with SDF-1	<i>In vivo</i> root canal of the dog	Dog pulp CD 105+, CD31 SP cells	Complete pulp-like tissue regeneration	Nakashima & Iohara (2011) [67]
Collagen with G-CSF	<i>In vivo</i>	hDPSCs human	Pulp-like tissue formation Differentiation of hDPSCs	Murakami, et al. (2013) [68]
Collagen	<i>In vitro</i>	hDPSCs human	Beneficial effect on proliferation and differentiation of hDPSCs	Kwon, et al. (2017) [69]
Collagen membrane	RCT	Regenerative endodontic procedure	promoted dentin formation in the middle third of the root wall	Jiang, et al. (2017) [61]

2.3 Acemannan, an extracted polysaccharide from *Aloe vera*

2.3.1 Aloe vera

Nowadays, herbal medicine is becoming popular, and it is recommended as a natural alternative in various treatments. Herbal products have been used in the treatment of various oral conditions and presently obtaining many scientific interests. Among them Aloe vera, a perennial succulent xerophyte, has a long history of

therapeutic uses worldwide. *Aloe barbadensis* Miller is the most biologically effective amongst 400 species of Aloe[70]. It consists of two different parts, the outer leaf layer and inner gel, with completely different compositions and therapeutic properties. Therapeutic benefits are mainly associated with clear gel in a central leaf pulp.

2.3.2 Active ingredients

More than seventy active ingredients from the inner gel of aloe vera leaf have been found (Table 4).

Table 4 active ingredients of *Aloe vera* leaf.

Table adapted from Arbaz et al. (2014)[71]

Class	Compounds
Vitamins	B1, B2, B6, C, A ($\beta\beta$ -carotene), choline, folic acid, $\alpha\alpha$ -tocopherol
Enzymes	Alkaline phosphatase, amylase, carboxypeptidase, catalase, bradykinase, cyclooxygenase, peroxidase, carboxypeptidase, cyclooxygenase, lipase, oxidase, phosphoenolpyruvate carboxylase, superoxide dismutase
Anthraquinones	Aloe emodin, aloetic acid, anthranol, aloin A and B (or collectively known as barbaloin), isobarbaloin, emodin, ester of cinnamic acid
Inorganic compounds	Calcium, chlorine, chromium, copper, iron, magnesium, manganese, selenium, zinc, potassium, phosphorous, sodium
Carbohydrates	Pure mannan, acetylated mannan, acetylated glucomannan (acemannan), galactan, glucogalactomannan, galactogalacturan, galactoglucoarabinomannan, arabinogalactan, pectic substance, xylan, cellulose
Saccharides	Mannose, glucose, L-rhamnose, aldopentose
Organic compounds and lipids	Arachidonic acid, $\gamma\gamma$ -linolenic acid, steroids (campesterol, cholesterol, $\beta\beta$ -sitosterol), triglycerides, triterpenoid, gibberellin, lignins, potassium sorbate, salicylic acid, uric acid

2.3.3 Acemannan

Acemannan is a major polysaccharide found in the inner leaf of the *Aloe vera* plant. It is comprised chiefly of mannose, glucose, and galactose monomers (fig 5).

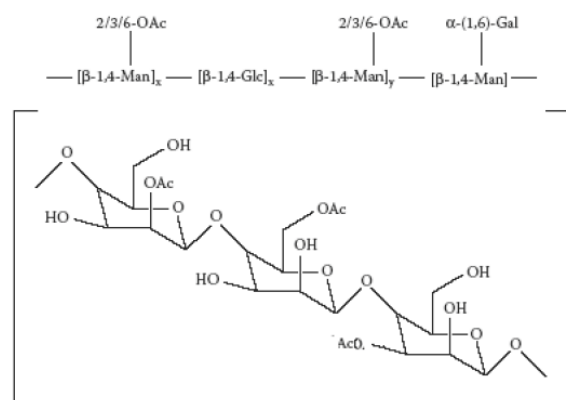


Figure 5 Structure of the mucopolysaccharide acemannan, extracted from *Aloe vera*. It is Beta-(1,4)-acetylated polymannose.

Photo courtesy from Sierra-García et al. (2014) [72].

2.3.4 Isolation and characterization of Acemannan

Acemannan can be isolated from the aloe vera gel with the various methods. Water extraction is the most used and convenient method. Table 5 shows the summary of various studies of acemannan.

Table 5 Summary various studies of acemannan

Source	Extraction, Fractionation, Purification	Structural Characterization Method	Monosaccharide Composition	Yield	Reference
Fresh gel	Water extraction (Homogenization, centrifugation mixed with 3 volumes of ethanol, lyophilization)	LC; FT-IR; SEC; ¹ H-NMR	Man: Glc: Gal = 57:22:17	---	Chokboribal, et al. (2015)(75)
Fresh gel	Water extraction; separation (Shodex Sugar KS-804 column)	¹³ C-NMR; SEM ¹ H-NMR; FT-IR	Man: Glc: Gal = 65:17:17	0.04%	Thunyakitpisal et al (2017)(76)
Frozen gel	Ultrafiltration cell membrane (Fractionated by ultrafiltration cell with MW cut-off membrane)	HPLC (BIOSEP SECH400 column); GC (SP2330 glass-capillary column); ¹ H-NMR; IR	Man: Glc = 97:3	2%	Lee et al (2001)(77)
Fresh gel	Water extraction; separation (homogenization, centrifugation, alcohol precipitation, dialysis, lyophilization)	HPLC (Shodex Sugar KS-804 column); GC-MS; ¹³ C-NMR	Man (77.18%); Glc (15.3%); Gal (4.9%); Ara (0.7%); Rha (0.2%); Fuc (0.34%); Xyl (0.7%)	0.2%	Boonyagul, et al. (2014)(78)
Fresh gel (1 year old)	Water extraction (Homogenization, centrifugation with 80% v/v alcohol, ammonium sulfate precipitation, lyophilization)	GC-MS; SEC; ¹³ C-NMR	Man: Glc = 15:1	---	Shi, et al (2018)(79)
Fresh gel	Water extraction; (Homogenization, centrifugation mixed with 3 volumes of ethanol, wash with ethanol, lyophilization)	HPGPC; FTIR; GLC-MS; TGA	Mannose (84.9%); glucose (7.2%); galactose (3.9%)	---	Khuma, et al. (2019)(80)
Frozen gel	Water extraction (Homogenization, centrifugation, alcohol precipitation, lyophilization)	GC-MS; Ion-chromatograph; ¹³ C-NMR	Man: Glc: Gal: GalA: Fuc: Ara: Xyl = 120:9:6:3:2:2:1	---	Tai-NinChow, et al. (2005)(81)
Fresh gel (3 years old)	Water extraction (Homogenization, centrifugation, supernatant mixed with 3 volumes of ethanol, pellet)	FACE; FT-IR; SEC	Man (62.9%); Glc (13.1%); Gal (0.6%)	1.7%	Khuma and Tiku (2016)(82)
Frozen gel	Water extraction; (depigmentation, deproteinization)	CR; GC-MS; PACE	Man (86.87%); Glc (0.05%); Gal (12.68%); Ara (0.38%)	0.32%	Quezada, et al. (2017)(83)

This table was adapted from Liu, et al. (2019)[73],[74], [75], [76], [77], [78], [79], [80], [81], [82]

2.3.5 Acemannan in dentistry

A lot of studies elucidated that acemannan has many biological activities such as, immunomodulation, anti-cancer, and antioxidant, gastric and intestinal, neuroprotective, and hepatoprotective activities[81-86]. Acemannan is also famous as wound healing agents and used in many biomedical applications, including dental

conditions such as apthous ulcer and alveolar osteitis[87, 88]. Acemannan is well known for its biological activities in periodontal tissue regeneration and bone regeneration (Table 6).

Table 6 Bioactivity of acemannan in dentistry

Cell type	Bioactivity	Action or Mechanism	Reference
Human gingival fibroblasts	Oral wound healing	Proliferation (+); keratinocyte growth factor-1 (KGF-1) (+); VEGF (+); type I collagen production (+)	Jettanacheawchankit et al. (2009) [89]
Human gingival fibroblasts	Oral wound healing	IL-6 (+); IL-8 (+); p50/DNA (+); TLR5/NF-KB (+); Binds with TLR5 ectodomain flagellin recognition sites	Thunyakitpisal et al. (2017) [75]
Bone marrow stromal cell (BMSC) (rat)	Periodontal tissue regeneration	BMSC proliferation (+); vascular endothelial growth factors (VEGF) (+); ALPase activity (+); bone morphogenic protein-2 (BMP-2) (+); bone sialoprotein (BSP) (+); osteopontin(OPN) (+); mineralization (+)	Shi et al. (2017)[90]
Human periodontal ligament cells	Periodontal tissue regeneration	Cell proliferation (+); RUNX2 (+); GDF5(+); VEGF (+); BMP2 (+); COL1 (+); ALP (+); mineral deposition (+)	Chantarawaratit et al. (2014)[91]
Human periodontal ligament cells, pulpal cells	Periodontal regeneration	BMP2 mRNA (+) and protein (+)	Jittapiromsak et al. (2010)[92]
Human primary dental pulpal cells	Dentin regeneration	Proliferation (+); alkaline phosphatase (+), type I collagen (+); BMP-2 (+); BMP-4 (+); vascular endothelial growth factor (+); dentin sialo protein expression (+); mineralization (+)	Songsiripraduboon et al. (2017) [8]

2.3.6 Role of acemannan in pulp tissue regeneration

For pulp tissue regeneration, the injured pulp is healed by the proliferation of pulp cells and the formation of the new pulp tissue. In 2004, Jittapiromsak *et al.* proved that acemannan significantly stimulated primary dental pulp cell proliferation and stimulated ALPase activity, BMP- 2, and DSP production *in vitro* and confirmed the acemannan activity dentin formation *in vitro* [93]. Alkaline phosphatase (ALPase) activity and dentin sialoprotein (DSP) are odontoblast differentiation markers and play an important role in mineral deposition. Songsiripradubboon *et al.* (2017) showed acemannan using as direct pulp capping material induced dentin bridge formation in primary human teeth and suggested that acemannan is an alternative biomaterial for vital pulp therapy[94]. Maintaining the pulp vitality in immature permanent teeth is the most important for continued root formation. Acemannan induced dentin bridge formation, which covered the pulp exposure site, and continued root formation in vital pulp therapy of immature permanent teeth[95]. Thus, acemannan could be the potential biomaterial for pulp tissue regeneration.

Chapter III

Materials and methods

In this research project, the material and methods part can be divided into 5 parts according to objectives:

- I. Extraction and characterization of porcine skin collagen
- II. Extraction and characterization of acemannan
- III. Preparation of acemannan-collagen scaffolds (AceCol scaffold)
- IV. Physical characterization of AceCol scaffolds
- V. Biocompatibility and biological activity of AceCol scaffold

Part I. Collagen extraction and characterization

1.1 Extraction of collagen from porcine skin

Porcine skin collagen was extracted in this study. Collagen was normally found in the dermis of the skin, so epidermis and subcutaneous tissue were removed during the extraction process. Porcine skin collagen was extracted by the previous publication method described by Nalinanon et al., (2007) with some modifications [96]. At first, the fresh porcine skin was obtained from the local market (Samyan market, Bangkok) and washed with tap water. After hair removal, the skin was treated with 0.1M NaOH to remove the proteins and lipids. Pretreated skin was incubated with 0.3 M acetic acid and 20,000 units/g pepsin (Sigma Aldrich, USA). The supernatant solution was precipitated with ice-cold 3M NaCl. Precipitants were collected, dialyzed against deionized water, freeze-dried, and kept at desiccator until use. All processes were performed at 4°C.

1.2 Characterization of the extracted porcine collagen

1.2.1 Total amino acid analysis

Collagens are the only animal proteins with a high content of hydroxyproline. The hydroxyproline content of extracted collagen is around 13.4 ± 0.24 percent [97]. Thus collagen could be measured through hydroxyproline[98].

The total amino acid was analyzed using the HPLC- precolumn-ACCQ Tag (Central Instrument Facility, Faculty of Sciences, Mahidol University, Thailand). Briefly, the sample was solubilized with 6M HCL and heated at 110°C for 22 hours. The solution was filtered with a 0.45 um membrane filter. The filtrate was then mixed with AccQ-fluor derivatization buffer and AccQ-fluor reagent to derivatize. The sample was heated at 55°C for 10 minutes and injected into HPLC. The amino acid standard (Sigma Aldrich, USA) was used as an internal control.

1.2.2 SDS-PAGE analysis

SDS-PAGE is an electrophoresis method to separate protein by its molecular weight using SDS (sodium dodecyl sulfate). Proteins are denatured and solubilized by binding with SDS along with the bit of boiling and reducing agents: dithiothreitol (DTT) or 2-mercaptoethanol. Thus, proteins form negatively charged complexes. When a constant electric field is used, the proteins transfer towards the anode, each with a different speed, depending on its mass through a sieve-like matrix of polyacrylamide gel [99].

SDS-PAGE was done by the method of Laemmli (1970)[100]. Samples were mixed with SDS-sample buffer (0.5M TrisHCl with 6%SDS, 6mM EDTA, 10% glycerol, and 0.05% Bromphenol blue, pH 6.8). The mixture had been heated at 95°C for 5 minutes and quickly cooled at 4°C in an icebox. The samples were loaded into a polyacrylamide gel (7.5% separating gel and 4% stacking gel) and then run at a constant current of 20 mA. The gels were then fixed with a mixture of 40% (v/v) methanol and 10% (v/v) acetic acid for 30 min wash and stained with 0.05% (w/v) Coomassie Blue R-250 in 15% (v/v) methanol and 5% (v/v) acetic acid for 1 h. Finally, they were destained with a mixture of 30% (v/v) methanol and 10% (v/v) acetic acid for 1 hour until the clear band was observed. High-molecular-weight protein markers (Pageruler Prestain protein marker, Thermofisher, USA) were used to calculate the molecular weight of the extracted collagen.

1.2.3 Western blot analysis

Western blotting is the transfer of proteins from the SDS- PAGE gel to a solid supporting membrane. Western blot analysis (antigen labelling) is performed

according to Timmons and Dunbar (1990) [101]. The proteins from the SDS-Page gel were transferred at 30 V overnight to an Immuno-Blot polyvinylidene difluoride (PVDF) membrane (0.2 μ m) with a wet transfer system, Bio-Rad blotting equipment. After transfer, membranes were incubated with non-fat dry milk (5% in 1x TBST) for 1 hour to block non-specific proteins. The primary antibody used was rabbit anti-collagen type I (Novus), whereas the secondary antibody is horseradish peroxidase-conjugated rabbit IgG (R&D system). The primary and secondary antibodies were diluted in the 1:1,000 blocking solution. Colour associated with antigen labeling was developed using ImmunoCruz western blotting luminol reagent provided with the kit.

1.2.4 CD spectrophotometer

CD spectroscopy is used for the study of the secondary structure of the proteins. CD detects absorption of right and left circularly polarized light by the proteins [102]. The collagen sample (0.5 g) was sent to Central Instrument Facility, Faculty of Sciences, Mahidol University, Thailand. Briefly, the sample was wavelength scanned using an Aviv model 400 spectrometer (Aviv Biomedical, Lakewood, NJ, USA). The positive ellipticity band at 222 nm and negative band around 195 nm was used to determine a triple-helical assembly of native collagen.

Part II. Extraction and characterization of acemannan

Acemannan was extracted from *A. vera* (*Aloe barbadensis* Mill.) leaves as previously described [74],[103]. After removing leaf skin, the pulp is washed with deionized water to remove yellow sap. The clear pulp was then homogenized and centrifuged. The supernatant was collected and precipitated with three volumes of absolute ethanol overnight. The resulting precipitate was collected by centrifuging and lyophilized. The white extract was characterized by FTIR to confirm as acemannan.

Part III. AceCOL scaffold preparation

The mixture of extracted collagen solution and acemannan was prepared as 1, 1:0.1, 1:0.2, and 1:0.4 (w/w) in a 100 mm diameter plastic plate, and then lyophilized to obtain the scaffolds as Col, Acecol 1, Acecol 2, and Acecol 3 scaffolds, respectively (Table 7).

Table 7 Composition and abbreviations of scaffolds

Composition(w/w ratio)	Abbreviation
Collagen	Col
Collagen + Acemannan (1:0.1)	AceCol 1
Collagen + Acemannan (1:0.2)	AceCol 2
Collagen + Acemannan (1:0.4)	AceCol 3

Part IV. Physical characterization of AceCol scaffold

4.1 Morphological analysis

SEM is used to analyze the scaffold morphology. The Col, AceCol 1, AceCol 2, and AceCol 3 Scaffolds were cut in mid-vertical and horizontal direction. The samples were fitted on stubs and sputtered with gold for 2 min at 20 mA with the vertical, and horizontal surface facing up. The scaffolds were viewed using Quanta 250 FEG scanning electron microscope (FEI, Oregon, USA).

4.2 Contact angle measurement

Contact angle of collagen and acemannan-collagen scaffolds (n=4) were measured using contact angle goniometer (Rameo-Hart, Newersy, USA) as previously described[104]. Briefly, each sample was dissolved in DMSO (4mg/ml), dropped into glass slide, and incubated at 65°C for 24 h to make a film. The films were dipped in distilled water, absolute alcohol and air-dried. Water contact angle was measured by dropping a water on the films.

4.3 Swelling test

The 6 mm diameter circular-shaped collagen and AceCol scaffold scaffolds (n=4) were prepared and weighted (Wd). After that, the samples were immersed in phosphate-buffered saline (PBS; pH 7.4) at 37°C, and weighted (Wt) in 15-, 30-, 45-, 60-, 180- min, and finally 24 h. The percentage of swelling was calculated following the formula.

$$\text{Swelling ratio (\%)} = [(Wt - Wd) / Wd] * 100$$

Wt = wet weight of the sample when t=15-, 30-, 45-, 60-, 180- min, and 24 h,

Wd = dry weight of the sample

4.4 Degradation test

The 6 mm diameter circular-shaped collagen and acemannan-collagen scaffolds (n=4) were prepared and weighed as initial weight (Wi). The samples were submerged in PBS (pH 7.4) at 37°C, and collected on days 1, 7, 14, and 30 post-incubation. The scaffolds were put on the filter to remove extra water and lyophilized. The final weight of samples (Wf) was recorded. The percentage weight loss of the sample was determined following the formula.

$$\text{Weight loss (\%)} = [(W_i - W_f) / W_i] * 100$$

4.5 Fourier-transform infrared spectroscopy (FTIR) analysis

The extracted collagen, acemannan, and acemannan-collagen scaffolds were grounded with KBr and evaluated the IR spectra using an FTIR spectrometer (Spectrum System 2000; PerkinElmer, Waltham MA, USA) at a wavenumber of 500-3800 cm⁻¹ with 64 scans/spectrum.

Part V. In vitro biocompatibility and biological activity of AceCol scaffolds

5.1 Cell culture

All cell culture reagents were purchased from Gibco, Invitrogen Corporation, CA, USA. Dental pulp cells were isolated from healthy pulp tissues obtained from intact third molars extracted at the Department of Surgery, Faculty of Dentistry, Chulalongkorn University. The protocol for human research was approved by the Ethical Committee, Faculty of Dentistry, Chulalongkorn University (HREC-DCU 2021-040), Thailand. Primary human dental pulp cells were cultured in the growth culture media (Dulbecco's modified medium (DMEM) supplemented with 10% fetal bovine serum (FBS) and antibiotic-antimycotic at 37°C, 5% CO₂ condition. All experiments used the third to seventh cell passage.

5.2 MTT and ELISA

In vitro cytotoxicity test of the scaffolds was determined using methyl-thiazol-tetrazolium (MTT) assay as previously described[105]. Briefly, the Col, AceCol1, AceCol2, and AceCol3 scaffolds were sterilized with gamma irradiation (Thailand Institute of Nuclear Technology, Thailand). The scaffolds were incubated in 2% FBS

DMEM at 37°C for 24 h. The conditioned media of the scaffolds was collected and passed through 0.2 µm sterile filter (Minisart Syringe Filter, Satorius, Germany). The dental pulp cells (25,000 cells per well) were seeded in a 48-well tissue culture plate (Nunc, Thermo Scientific Fisher, USA) for 24 h at 5% CO₂ and 37°C incubator. The cells were washed with phosphate buffer saline and then treated with the conditioned medium for additional 24 hours. Control wells were treated with the same volume of 2% FBS supplemented DMEM media. After that, the cells were incubated with 1 mg/mL MTT solution for 30 minutes. The precipitates were dissolved in dimethyl sulfoxide, and the light absorbance was measured at 570 nm. The experiment is 3-times independently repeated.

For ELISA, the pulp cells treated with the conditioned medium for an additional 72 h. Control groups were treated with the same volume of 2% FBS supplemented DMEM media. After that, the conditioned media from the Col, AceCol1, AceCol2, and AceCol3 treated groups were collected at 24 and 72 h for VEGF and BMP-2 measurement using ELISA kits (R&D System, Minneapolis, USA) following the manufacturer's instructions. The sensitivity for VEGF and BMP-2 were 8.4 and 11 pg/ml, respectively.

5.3 SEM

The 10x10 mm fabricated scaffolds were soaked in the growth culture media for 30 min and placed in the 8-wells cell culture slide (SPL Life Science, Korea). The 3x10⁴ dental pulp cells are seeded on the scaffolds and incubated for 1, 3, 7, and 14 days. The scaffolds were rinsed 3 times with PBS (pH 7.4) and fixed with 2.5% glutaraldehyde in PBS. The samples were dehydrated with serial ethanol dilutions, critical point drying, and gold coating. The scaffolds were then evaluated for cell morphology, cell-cell interaction, and cell-material interactions via SEM.

5.4 Immunofluorescence evaluation

The osteogenic protein (osteopontin (OP; Abcam, Cambridge, UK), bone sialoprotein (BSP; Abcam, Cambridge, UK), and dentin sialophosphoprotein (DSPP; Invitrogen, Thermo Fisher Scientific, MA, USA) expressions were examined using immunofluorescence staining technique. The 10x10 mm fabricated scaffolds were

soaked in the growth culture media for 30 min and placed in the 8-wells cell culture slide (SPL Life Science, Korea). The 3x10⁴ dental pulp cells are seeded on the scaffolds and incubated for 3 days. The scaffolds were fixed with 2.5% glutaraldehyde, cut in mid-vertical, embedded in vertical and horizontal surface facing up, and frozen. The scaffold samples were then cryosectioned at 10 micrometre thickness, transferred to positively charged microscope slides, and dried. The scaffolds were rinsed with PBS, permealized with 0.2% Triton X-100, and blocked with 5% skim milk for 30 minutes at 37°C. The sections were incubated with primary antibodies (1:200 dilution) overnight at 4°C, and then secondary antibodies conjugated with Alexa Fluor[®] 488, 647, and 568 (1:200; Abcam, Cambridge, UK) for additional 2 hours. Finally, the slides were counterstained with 4, 6-Diamidino-2-Phenylindole (DAPI, Invitrogen, Thermo Fisher Scientific, MA, USA). The FV3000 confocal laser scanning microscope with software version 3.3 (Cellsense Olympus, Tokyo, Japan) was used to view the sections.

5.5 Calcium concentration measurement

After cultured for 3- and 7-days, the scaffolds (n=4) were fixed with 2.5% glutaraldehyde, washed with distilled water, and freeze-dried. The samples were dissolved in 1% nitric acid at 120°C for 2 h and then 37°C for couple days. The conditioned solution was filtered and evaluated for calcium concentration using ICP-OES optical emission spectrometer (PerkinElmer, Waltham MA, USA).

5.6 Computational simulations

5.6.1. Structure models of acemannan and collagen compounds

The simulated single stand, sixteen monosaccharide length acemannans SAC1 (C₁₄₄H₂₂₆O₁₁₃; 483 atoms) and SAC2 (C₁₂₈H₁₉₄O₉₇; 419 atoms) as a ligand compound were made based on our previous model [106] and the simplest non-branching acetylated D-mannose units, respectively. The optimized structures of SAC1 and SAC2 were created using a semi-empirical AM1 method [107] and the Gaussian 09 program package [108]. Dipole moments of SAC1 and SAC2 were also evaluated (fig. 6a and 6b). The triple helix type I collagen (COL) was obtained from the PDB ID-1CGD

[109] (fig. 6c). The molecular graphics of these simulated model were visualized using the UCSF Chimera [110].

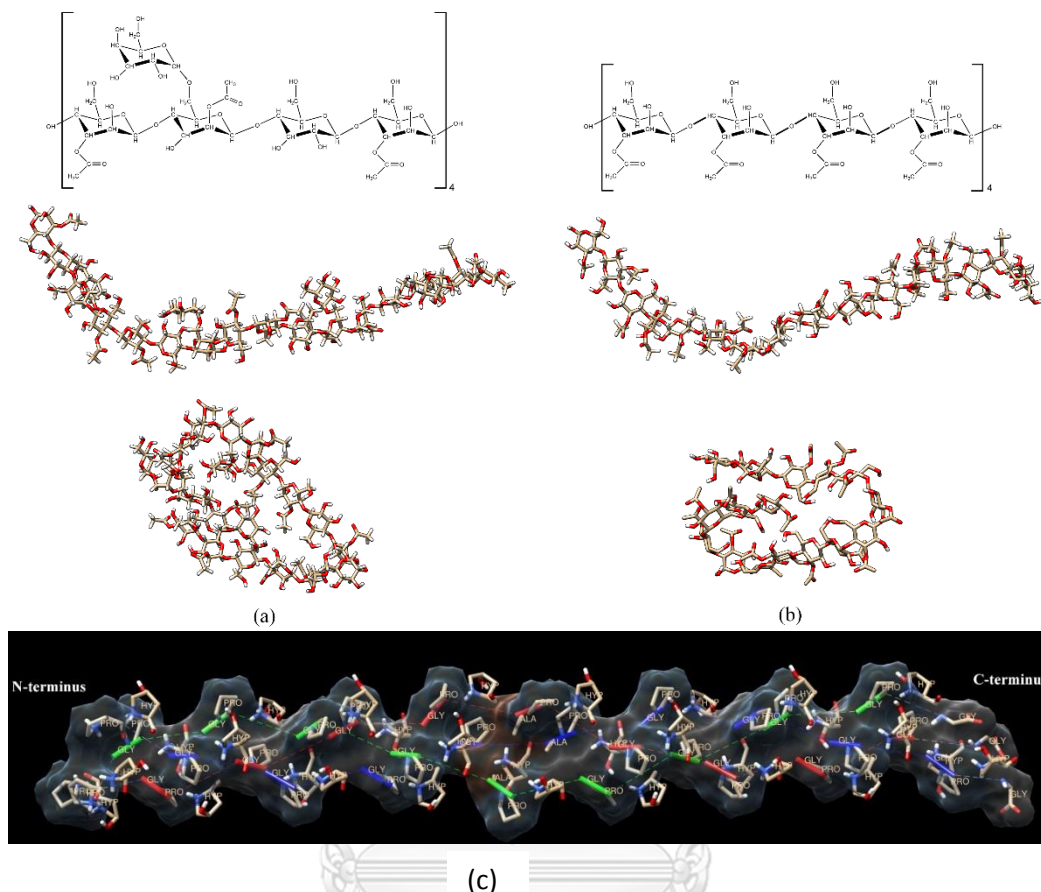


Figure 6 Molecule of acemannan (a) SAC1 and (b) SAC2 model. Top, middle, and bottom images are structural formula, AM1-optimized structures, and the highest binding affinity form to bind collagen which based on molecular docking algorithm, respectively. (c) molecular structure of the collagen type I (COL) with hydrophobicity surface. The COL was taken from the PDB [109]. The graphic was visualized by the program UCSF Chimera [110].

5.6.2 Docking simulation and details

To investigate the interaction between acemannan and collagen at the atomic level, SAC1 and SAC2 were docked onto COL to form SAC1-COL and SAC2-COL, respectively. After that, the second SAC1 and SAC2 ligands were docked at SAC1-COL and SAC2-COL to form SAC1-(SAC1-COL) and SAC2-(SAC2-COL) complex, respectively. All molecular dockings were performed using AutoDock Vina [111, 112].

Statistical Analysis

The data were collected and presented as mean \pm SD for contact angle, swelling, degradation rate and calcium concentration, and as mean \pm SE for cell viability, VEGF, and BMP-2. The data between each group was analyzed by one-way analysis of variance using the SPSS program for Windows, version 22 (SPSS, Inc., Chicago, IL, USA). The multiple comparison test was used for post-hoc analysis. Independent *t*-test was performed to evaluate calcium calcification. Significance was assumed at $p < 0.05$.



Chapter IV

Results

4.1 Porcine skin collagen extraction and characterization

The starting weight of porcine skin was 800g and final weight of our extract was 140g so the extract yield was 17.5% (w/w). Total amino acid analysis reported that the extract was mainly composed of glycine (18%), proline (10.7%), glutamic acid (9.2%), and hydroxyproline (9%) (Table 8). Using anti-Type I collagen antibody, the immunoblot demonstrated two protein bands at 130 kDa for α_1 and α_2 chains, and 180 kDa for β chain of collagen, which is a duplex form of alpha chains (Fig 7a). The CD spectroscopy shows clear transitions, including a positive band at 222 nm and a negative band around 196 nm (Fig 7b) [113]. FT-IR exhibited amide I (1700-1600 cm^{-1}), amide II (1600-1500 cm^{-1}), and amide III absorptions (1250-1350 cm^{-1}) as the marker signal of collagen where the mean frequency at 1630 and 1660 cm^{-1} for triple helix contribution and α -helical structure, respectively [114] (Fig 8).

Table 8 Percentage amino acid composition of the extracted porcine skin collagen.

Amino acids	mg%
Hydroxyproline	8.98
Aspartic acid	5.38
Serine	2.98
Glutamic acid	9.22
Glycine	18.06
Histidine	0.42
Arginine	2.00
Threonine	4.22
Alanine	7.31
Proline	10.68
Tyrosine	0.19
Valine	2.07
Lysine	3.41
Isoleucine	0.98
Leucine	2.26
Phenylalanine	1.39

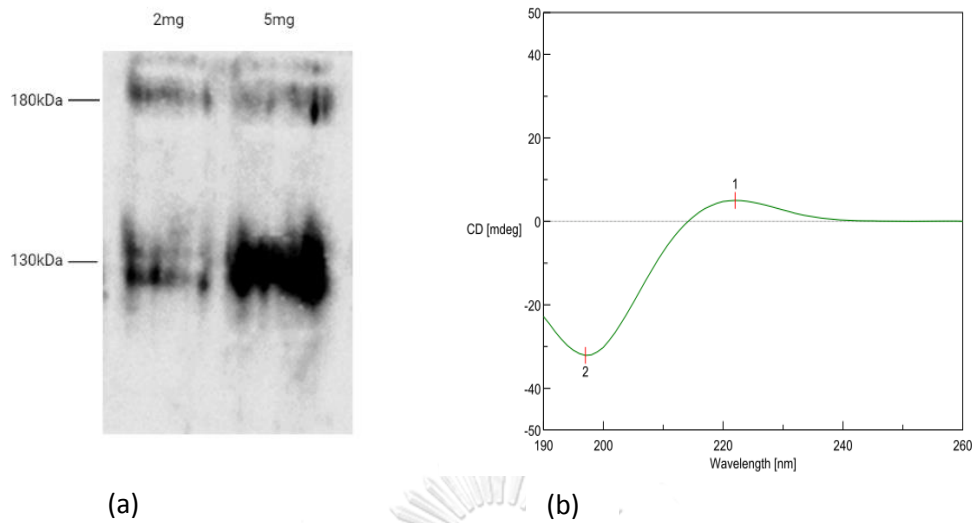


Figure 7 The extracted collagen was characterized using (a) immunoblot analysis of 2 and 5 mg of the protein (b) Circular dichroism (CD) spectroscopy of the extracted collagen. The negative and positive bands are detected at 197 and 222 nm, respectively.

4.2 Characterization of the AceCol scaffolds

The FT-IR of collagen, acemannan, and AceCol were demonstrated (Fig 8). FTIR analysis of the representative collagen and acemannan-collagen scaffolds demonstrated the peak of carbonyl group of acemannan (1740), amide groups of collagen (1679, 1542, and 1238 respectively).

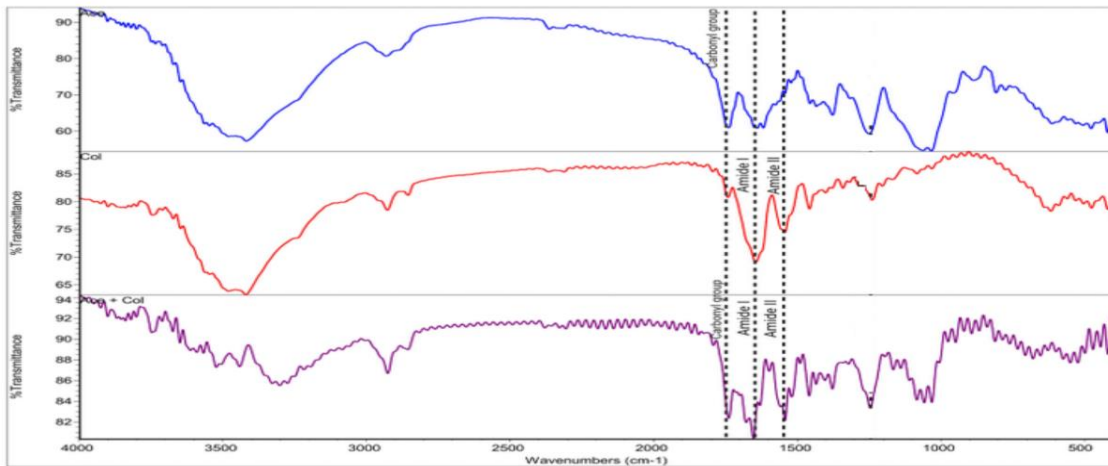
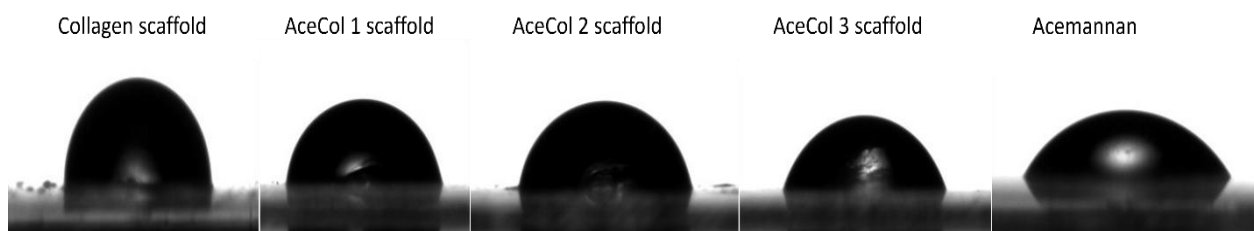


Figure 8 FTIR analysis of the representative collagen and acemannan-collagen scaffolds demonstrated the peak of carbonyl group of acemannan (1740), amide groups of collagen (1679 and 1542).

The water contact angle measurement revealed that the collagen scaffold and acemannan scaffold have the contact angles of $90.24^\circ \pm 5.54$ and $49.47^\circ \pm 6.06$. AceCol 1, AceCol 2, and AceCol 3 demonstrated the degree of contact angle at $76.24^\circ \pm 5.34$, $68.98^\circ \pm 2.51$, and $62.48^\circ \pm 6.63$ ($n = 4$), respectively, which is between that of collagen and acemannan (Fig 9 a). Swelling ratio of AceCol scaffolds significantly increased around 1.8-2 folds compared with that of collagen scaffold ($p < 0.05$; Fig 9b). The maximum swelling of the scaffolds was reached at 1 h post-incubation. Up to 2 months of observation, no significant difference in degradation rate was detected in all the scaffold groups, which implied acemannan does not alter collagen degradation rate (Fig 9c). Therefore, adding acemannan resulted in enhancing hydrophilicity and water absorption of AceCol scaffold in dose-dependent manner.



(a)

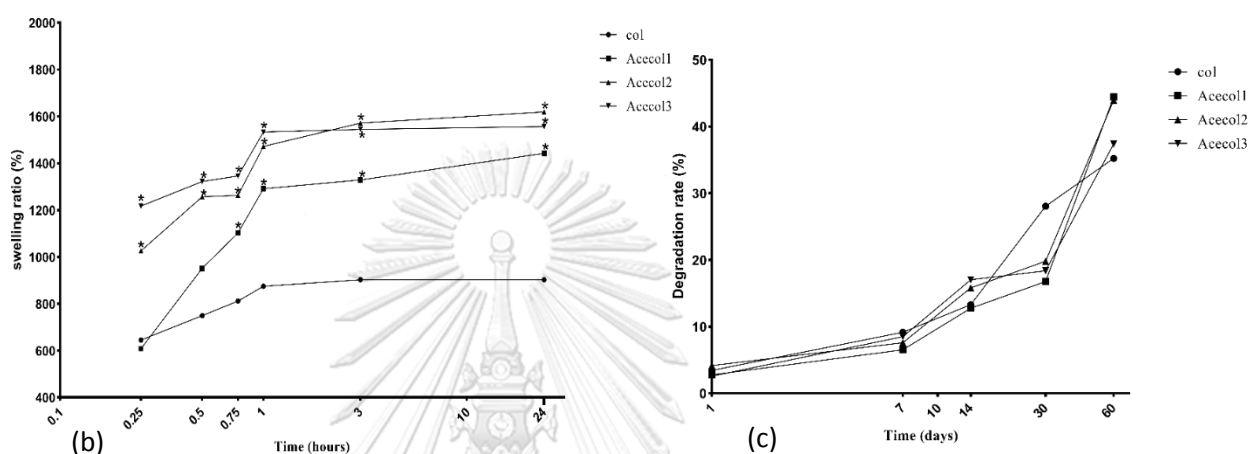


Figure 9 The representative collagen and acemannan-collagen scaffolds (a) Water contact angle measurement, (b) Swelling ratio, and (c) degradation rate. $N=4$. * Statistically significant difference from collagen, ($p < 0.05$).

4.3 Morphology analysis with SEM

SEM images revealed that both collagen and AceCol scaffolds resemble porous sponges with numerous three-dimensional interconnected pores. AceCol scaffolds have more densely arranged surface with increasing concentration of acemannan. In the vertical cross-section view, Acecol scaffolds have stacking sheet-like pattern and collagen scaffold has random honeycomb appearance (fig 10).

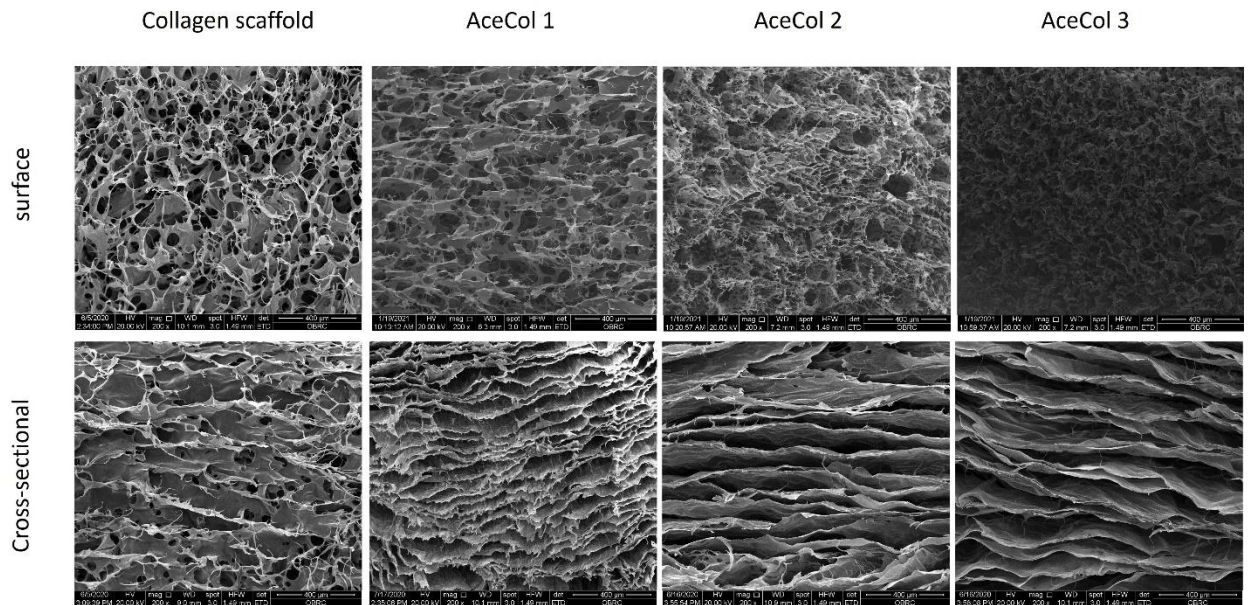


Figure 10 SEM images of scaffold morphology; collagen, AceCol 1, AceCol 2, and AceCol 3 scaffolds.

4.4 Biocompatibility and growth factors secretion of collagen and AceCol scaffolds

From MTT data, no cytotoxicity was observed in all Col and AceCol scaffolds. The condition media obtained from AceCol1 and AceCol2 significantly induced cell proliferation compared with the control group at 24 h ($p < 0.05$; Fig 11).

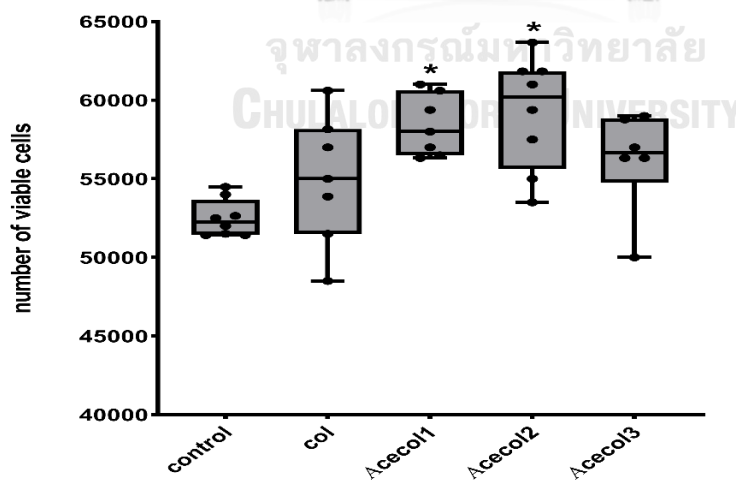


Figure 11 Cell viability at 24 h. Dental pulp cells were treated with the condition media of Col, AceCol1, AceCol2, and AceCol3. *, # Statistically significant difference from control and collagen groups, respectively ($p < 0.05$).

AceCol1 significantly enhanced BMP-2 and VEGF expression compared with the control group around 3.4 and 4.6 folds, and that of collagen at 2.5 and 1.2 folds, respectively ($p < 0.05$). AceCol2 significantly stimulated BMP-2 and VEGF expression compared with the control at 2.6 and 5.2 folds and that VEGF of collagen group around 1.3-fold, respectively ($p < 0.05$). AceCol3 significantly induced only VEGF expression compared with control around 3.1-fold ($p < 0.05$). The collagen scaffold group significantly increased BMP-2 and VEGF synthesis up to 1.8 and 3.8 folds, respectively, compared with the control ($p < 0.05$; Fig 12). Based on physical and biological activities information, the ratio of acemannan and collagen at 1:10 (w/w) could be an optimal concentration. Therefore, AceCol 1 scaffold was selected for further investigation.

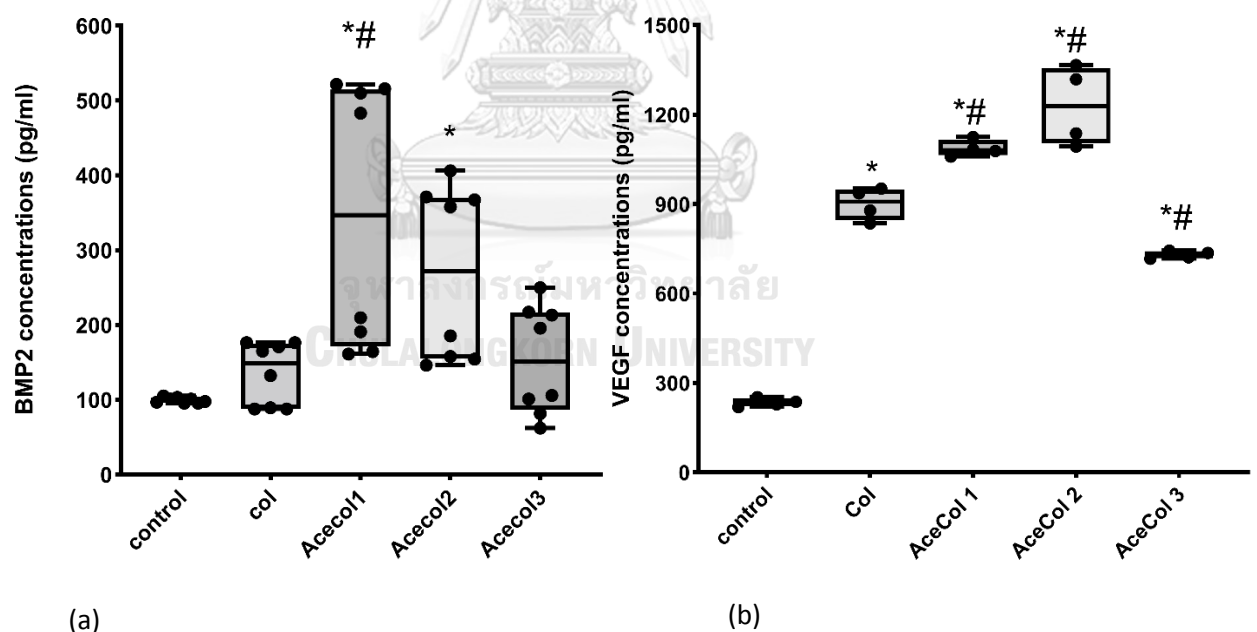


Figure 12 Dental pulp cells were treated with the condition media of Col, AceCol1, AceCol2, and AceCol3. (a) BMP2 at 72 h, and (b) VEGF expression at 24 h. *, # Statistically significant difference from control and collagen groups, respectively ($p < 0.05$).

4.5 Cell adhesion and extracellular matrix formation

The SEM images revealed that both lyophilized collagen and AceCol1 scaffolds resemble porous sponges with numerous three-dimensional interconnected pores (Fig 13). In the vertical cross-section view, the AceCol scaffold has a stacking sheet-like pattern while collagen scaffold has a random honeycomb appearance. Cell-scaffold adhesion and cell-cell interaction were observed at 4 h of incubation. From SEM and DAPI staining signal data, more cell numbers and extracellular matrix synthesis were detected in both collagen and AceCol scaffolds in time-dependent manner (Fig 13 and 14).

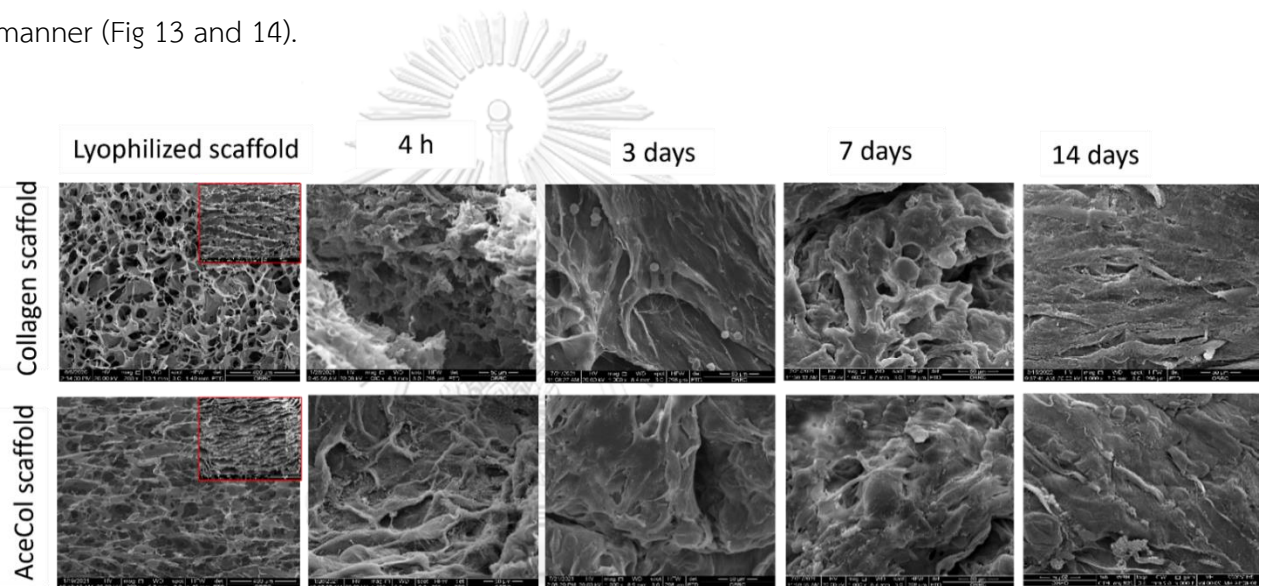


Figure 13 SEM images of human dental pulp cells attachment and the scaffold morphology at 4 h, 3 days, 7 days, and 14 days post-incubation on Col and AceCol1 scaffolds. Cells were seeded on the scaffold and cultured in growth culture media. The fresh media was replaced every couple day.

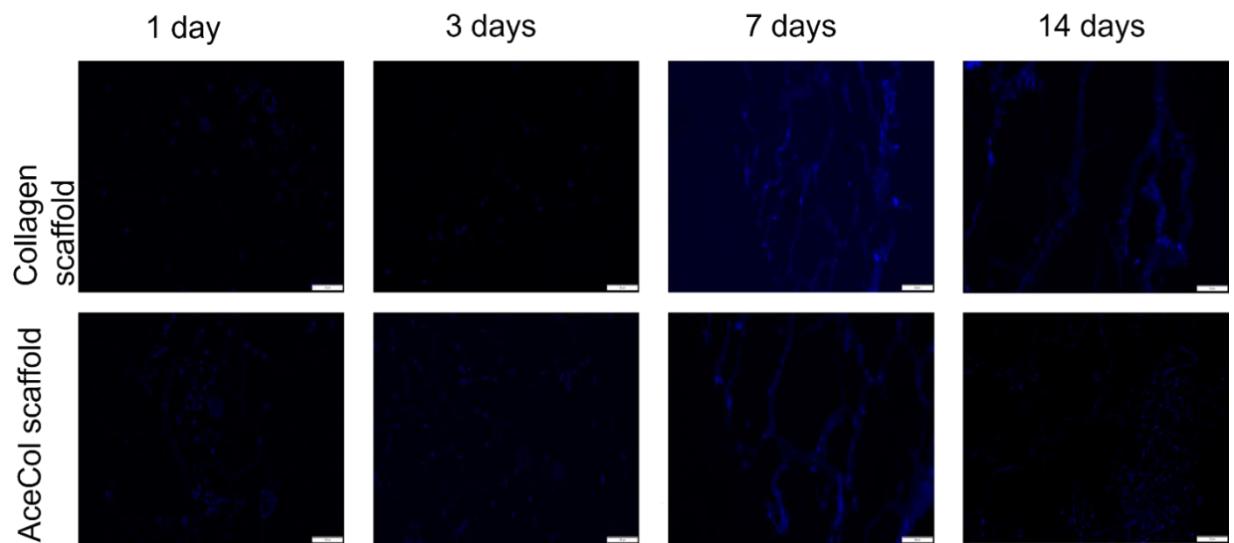


Figure 14 DAPI staining of the nucleus of the cells distributed over the scaffolds at 1 day, 3 days, 7 days, and 14 days post-incubation. Cells were seeded on the scaffold and cultured in growth culture media. The fresh media was replaced every couple day.

4.6 Immunofluorescence evaluation of osteogenic proteins expression

We detected BSP and OPN in both collagen and AceCol samples at 3 days of incubation (Fig. 15 a and b). Interestingly, DSPP expression was only detected in AceCol scaffold (Fig. 15 c).

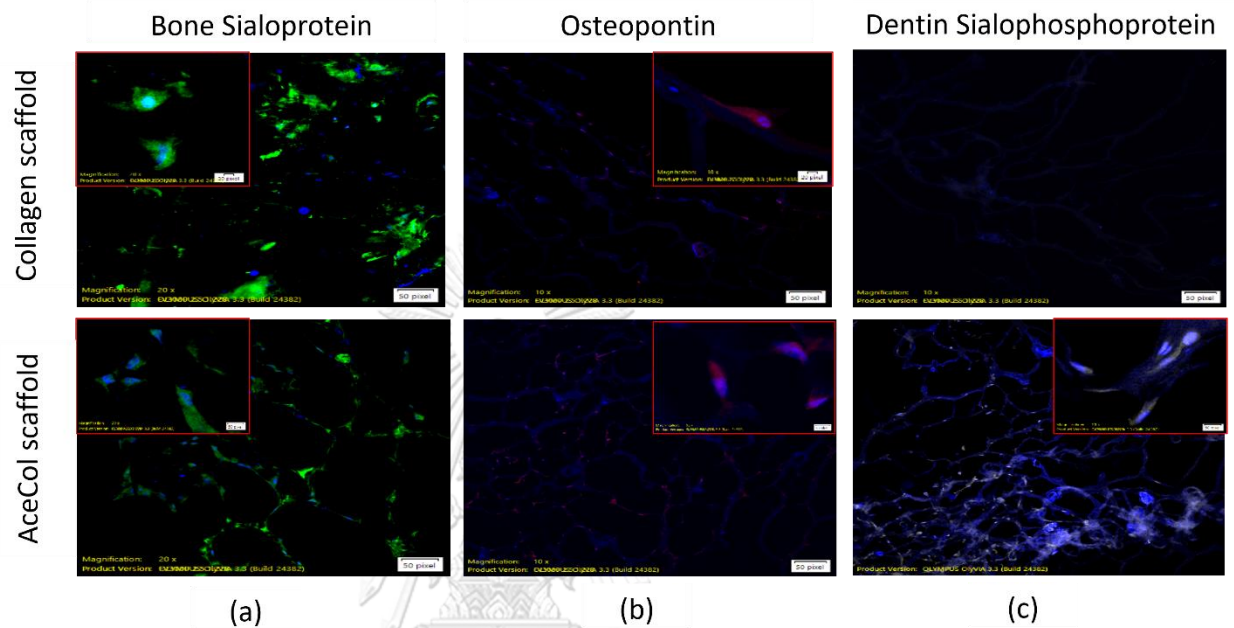


Figure 15 Osteogenic protein expressions were evaluated using immunofluorescence staining technique. Cells were seeded in Col and AceCol scaffolds and incubated for 3 days. (a) Bone sialoprotein (BSP) stained with Alexa fluor 488, (b) Osteopontin (OP) stained with Alexa fluor 647, and (c) Dentin Sialophosphoprotein (DSPP) stained with Alexa fluor 568. Cellular nuclei were counterstained with DAPI. Magnification x10. Insert image magnification x100.

4.7 Mineral deposition

To prevent the possibly interaction between dye and collagen protein, mineral deposition was assessed by calcium content of collagen and AceCol scaffolds after 7-days of culture. At day 7, the calcium concentration in the AceCol scaffolds was significantly ~ 7 -fold higher compared with the collagen scaffold (17.79 ± 6.16 mg/L and 2.55 ± 0.57 mg/L, respectively; $p < 0.05$). This data supports our previous finding, inductive effect of acemannan on mineral deposition in pulpal cell, bone marrow stromal cell, and periodontal ligament cell [91, 92, 115].

4.8 Computational simulation

Docking of SAC1 and SAC2 onto COL

From measurement, Dipole moments of SAC1 and SAC2 were 24.68 and 16.39 Debye, respectively. The nine modes binding energies (a-i) of the SAC1-COL, SAC1-(SAC1-COL), SAC2-COL, and SAC2-(SAC2-COL) complex were shown in Table 9. Interestingly, both SAC1 and SAC2 were altered their 3D configuration from linear to oval shape-liked structure. Based on the highest affinity binding, SAC1 and SAC2 ligands prefer to bind at the polar region of C-terminal of collagen (Fig.16 and 17). The binding energies of the first SAC1 and SAC2 molecules to COL are -3.9 and -3.6 kcal/mol, respectively (Table 9).

Table 9 Nine modes of the highest binding energies of single strand acemannan model: β -(1,4)-acetylated polymannose with β -(1,4) glucose and α -(1,6)-linked galactose side-chain (SAC1) and 1,4 glycosidic linkage of acetylated polymannose (SAC2) dock against collagen molecule (COL).

Docking system	Mode	R ^b		
		Affinity ^a	L-RMSD	U-RMSD
SAC1 - COL	1 ^c	-3.9	0.000	0.000
	2	-3.8	8.370	22.132
	3	-3.7	1.675	4.727
	4	-3.7	2.988	18.412
	5	-3.7	10.214	19.093
	6	-3.7	14.545	24.205
	7	-3.6	10.779	19.151
	8	-3.6	8.786	18.185
	9	-3.6	31.929	41.254
SAC1 ^c - (SAC1-COL)	1 ^d	-4.2	0.000	0.000
	2	-4.0	5.699	16.337
	3	-3.9	5.905	17.634
	4	-3.8	5.146	20.973
	5	-3.8	5.792	17.339
	6	-3.8	5.738	17.353
	7	-3.7	5.227	15.652
	8	-3.7	5.667	17.550
	9	-3.6	13.248	23.304
SAC2 - COL	1 ^e	-3.6	0.000	0.000
	2	-3.5	32.537	42.417
	3	-3.5	31.857	42.678
	4	-3.5	26.348	40.040
	5	-3.5	2.109	4.057
	6	-3.5	29.833	43.652

	7		-3.4	1.590	2.714
	8		-3.4	27.419	42.238
	9		-3.4	5.632	17.068
SAC2 – (SAC2/COL)	1 ^f		-3.3	0.000	0.000
	2		-3.2	1.511	2.144
	3		-3.2	13.713	21.573
	4		-3.1	3.673	11.232
	5		-3.1	18.427	26.185
	6		-3.0	15.557	25.711
	7		-3.0	19.485	26.691
	8		-3.0	18.873	27.104
	9		-3.0	17.672	25.883

^a In kcal/mol.

^b Distance in Å from best mode, whereas L-RMSD and U-RMSD are lower and upper bound, respectively.

^{c,d,e,f} The highest affinity SAC1 docked against COL, SAC1 docked against SAC1-COL, SAC2 docked against COL, and SAC2 docked against SAC2-COL, respectively.

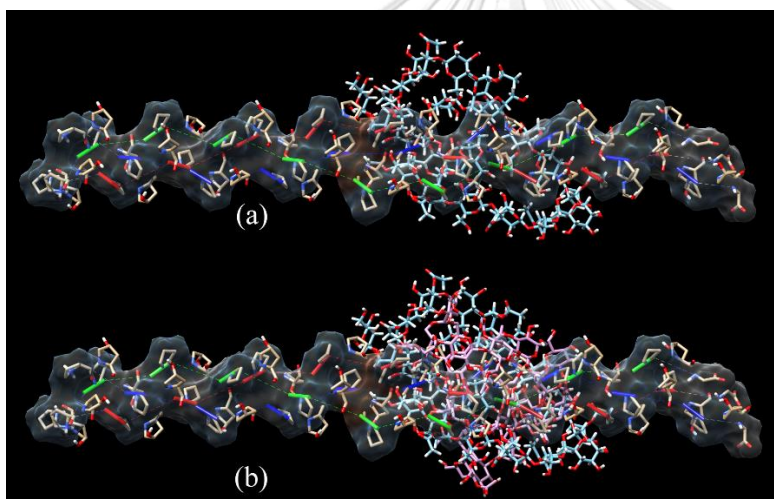


Figure 16 Graphical representation of (a) SAC1-COL complex based on the highest affinity of SAC1 binding to COL (b) SAC1-(SAC1-COL) complex obtained from the highest affinity of secondary SAC1 molecule binding to SAC1-COL complex. The binding energies of first and second SAC1 onto the COL and the SAC1-COL are -3.9 and -4.2 kcal/mol, respectively.

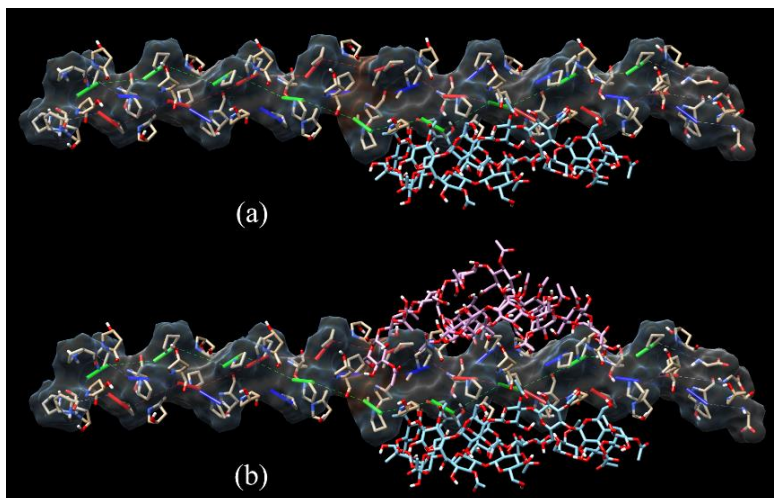


Figure 17 Graphical representation of (a) SAC2-COL complex obtained from the highest affinity of SAC2 binding to COL (b) SAC2-(SAC2-COL) complex based on the highest affinity of secondary SAC2 molecule binding to SAC2-COL complex. The binding energies of first and second SAC2 onto the COL and the SAC2-COL are -3.6 and -3.3 kcal/mol, respectively.

For the new coming acemannan molecules, both of the second SAC1 and SAC2 molecules prefer to bind, at least partially, to the SAC1 molecule of the SAC1-COL and SAC2 molecule of the SAC2-COL, respectively, rather than creating the new COL binding site. Many interaction configurations are observed, i.e., stacking dish pattern of primary and secondary acemannan ligands, partial stacking dish of primary and secondary acemannan with some parts of second ligand binding to COL, and sandwich with partial overlapping pattern. The highest binding energies of SAC1-(SAC1-COL) and SAC2-(SAC2-COL) are -4.2 and -3.3 kcal/mol, respectively (Table. 9).

Chapter V

Discussion

The choice of an appropriate scaffold is the first and important step to provide a suitable environment for regeneration. The ideal bioactive scaffold must have the characteristic similar to the native extracellular matrix and should offer a three-dimensional matrix for cell migration and proliferation. In this study, we extracted the collagen from porcine skin and acemannan from aloe vera leave. We then developed bioscaffold combined of those two extracts and characterized for pulp tissue regeneration.

The acid-enzyme extraction method has been acceptable to extract collagen which uses in biomedical applications[116]. In this study, the porcine skin was pretreated with $\text{Na}(\text{OH})_2$ to remove lipid and non-collagenous protein and the collagen was then extracted with enzyme pepsin in acidic condition for antigenic telopeptide elimination [117].

Our data revealed the extracted protein was composed of glycine, proline, glutamic acid, and hydroxyproline that are main components of collagen. Using anti-Type I collagen antibody, the immunoblot demonstrated protein bands for α_1 , α_2 chains, and β chain of collagen, which is a duplex form of alpha chains. The CD spectroscopy and FT-IR exhibited the marker signal of collagen for triple helix contribution and α -helical structure. Taken together, these obtained data confirm that the precipitant protein is a type I collagen with a secondary triple alpha-helix structure.

We prepared AceCol scaffolds (AceCol 1, AceCol 2, and AceCol 3) with different acemannan concentrations and characterized physically and biologically to determine optimal concentration. AceCol scaffold exhibited the peak of carbonyl absorption ($\text{C}=\text{O}$; $1710\text{-}1740\text{ cm}^{-1}$) and C-O-C stretching (1250 cm^{-1}) as the marker of acemannan, and the amide I, II, and III bands as the marker of collagen which confirms the composite scaffold contained both acemannan and collagen.

The surface hydrophilicity of the regenerated scaffold is critical for supporting cell attachment and adhesion[118]. In our study, the hydrophilicity of scaffolds was assessed by contact angle and swelling properties. As the structural supramolecule, the assembly of collagen fibrils needs a contact angle of more than 80 degrees for maintaining a hydrophobic exterior area and acemannan contact angle is around 40 degree [104, 119]. AceCol1, AceCol2, and AceCol3 demonstrated the degree of contact angle which is between that of collagen and acemannan. The swelling behavior of the scaffold is important for tissue regeneration. Increasing its pore size and volume via water absorption resulted in enhancing the amount of oxygen and nutrients accumulation, and then their exchange efficiency to support cell activity during tissue formation [120]. From our data, adding acemannan resulted in enhancing hydrophilicity and water absorption of AceCol scaffold in dose-dependent manner and acemannan does not alter the collagen degradation rate.

From MTT data, no cytotoxicity was observed in all Col and AceCol scaffolds. In addition, AceCol scaffolds significantly induced pulp cell proliferations. From SEM and DAPI staining signal data, cell-scaffold adhesion and cell-cell interaction were observed and more cell numbers and extracellular matrix synthesis were detected in both collagen and AceCol scaffolds in time-dependent manner. Taken together the above data, AceCol scaffold has biocompatibility and inductive effect on dental pulp cell proliferation confirming the finding of Jittapiromsak et al [92].

For pulp tissue regeneration, growth factors play a role in regulating vascular renewal and proliferation and odontoblast differentiation. VEGF and BMP-2 act synergistically for pulp regeneration. VEGF increases the renewal of vasculature in the early phase of healing and increased their proliferation, and BMP-2 regulates odontogenic differentiation and stimulates mineralization of the newly formed matrix essential for dentin-pulp complex regeneration [9, 10]. In the present study, our data suggest the cooperatively inductive effect of acemannan and collagen on BMP-2 and VEGF expression [8, 92, 121, 122].

BSP and OPN are extracellular non-collagenous matrix proteins detected in both bone and dentin, while DSPP has been considered as a distinctive marker for dentin [123]. Dentin forming cells secreted these proteins during differentiation and

dentin mineralization [124]. We detected BSP and OPN in both collagen and AceCol samples at 3 days of incubation. Interestingly, DSPP expression was only detected in AceCol scaffold. Expression of these matrix proteins elucidates biocompatibility and bioactivity of the AceCol scaffold in tissue regeneration. In addition, this data has supported the previous reports that acemannan induced DSPP expression and enhanced osteodentin bridge formation [92, 125].

Mineralization after cell proliferation and differentiation is also the important step in the regeneration process. In our study, mineral deposition was evaluated by calcium concentration measurement of cell seeded scaffolds after 3- and 7-days of culture. The calcium concentration was significantly increased in time dependent manner. The data supports our previous finding, inductive effect of acemannan on mineral deposition.

Due to the nature of collagen as a mostly hydrophobic and relatively rigid structure, acemannan has to alter to minimize its size from linear to oval-shape for binding into the small polar area of collagen to generate acemannan-collagen complex. This finding is similar to the interaction of collagen peptide with YKL-40 glycoprotein [126] and in case of collagen-pectin composite [127]. This polysaccharide-protein interaction would create the bigger hydrophilic polarity zone in collagen surface in which the second molecule of acemannan prefer to bind this location rather than finding the new site, resulted in increasing higher polarity region of the collagen. In addition, the steric hindrance of galactose sidechain would create more easily access for water to attach collagen. That is corresponded with our data that adding acemannan increases surface contact angle and hydrophilicity of the collagen. Moreover, this higher hydrophilicity area would be the preferential location for cell attachment [128] where acemannan has more opportunity near to the cell and activate them.

From computerized simulation model, SAC1-COL and SAC1-(SAC1-COL) has the higher binding energy rather than SAC2-COL and SAC2-(SAC2-COL), respectively. This finding suggested that β -(1,4)-acetylated polymannose with β -(1,4) glucose and α -(1,6)- galactose branching (SAC1 model) has a higher binding affinity to collagen

rather than that of β -(1,4)-acetylated polymannose (SAC2 model). The possibility explanation is SAC1 has the greater polarity than SAC-2. The branching of galactose in SAC1 which provide more four hydroxy groups (-OH) may make acemannan SAC1 more polarity and more chance to form a stable complex rather than that of non-branching acetylated D-mannose SAC2 model.

The precise underlying signaling pathway how acemannan stimulates cellular activity is still unclear. Mannose receptor has been proposed as one of acemannan's candidate receptor [89]. Xing et al. demonstrated acemannan induced fibroblast proliferation via cyclin D1 protein expression through AKT/mTOR signaling pathway [129]. Using computational program, glycosaminoglycan-acemannan has docked into TLR-2 receptor and then upregulated the downstream osteogenesis gene activity in bone marrow stromal cells[130-132]. Acemannan also binds to TLR5 receptor and activates nuclear protein NF-kappaB to upregulate IL-6/-8 expression[75].

Taking all evidence together, our data generate the knowledge of some physical properties and biological properties of acemannan-collagen scaffolds. This knowledge provide more understanding on usage of acemannan with collagen and it can be applied clinically for pulp tissue regeneration in the future.

Chapter VI

Conclusion

In this study, we investigated the effect of AceCol scaffolds on wettability, swelling, degradation, 3D morphology, biocompatibility, growth factor secretion, and extracellular matrix protein synthesis. Our data revealed that acemannan can improve the hydrophilicity and swelling ability, without altering the degradation rate of collagen scaffolds. According to our computational simulation data, the polar zone of the collagen is a preferential site for acemannan binding. Acemannan is able to modulate its 3D structure to bind to collagen and the other acemannan molecules using polarity interaction. Cooperation of acemannan and collagen also enhanced biological activities of dental pulp cells including adhesion and proliferation, VEGF and BMP2 secretion, BSP, OPN, and DSPP expression, and mineralized matrix formation in the better performance for pulp tissue regeneration. For the translation of these laboratory findings to clinical application, further *in vivo* and clinical studies of this material should be performed. In conclusion, the AceCol scaffold is a promising material for tissue regeneration.

REFERENCES



จุฬาลงกรณ์มหาวิทยาลัย
CHULALONGKORN UNIVERSITY

1. Rizk, H.M., M.S.M.S. Al-Deen, and A.A.J.T.S.D.J. Emam, Comparative evaluation of Platelet Rich Plasma (PRP) versus Platelet Rich Fibrin (PRF) scaffolds in regenerative endodontic treatment of immature necrotic permanent maxillary central incisors: A double blinded randomized controlled trial. 2020. 32(5): p. 224-231.
2. Glowacki, J. and S. Mizuno, Collagen scaffolds for tissue engineering. *Biopolymers*, 2008. 89(5): p. 338-44.
3. Irawan, V., et al., Collagen Scaffolds in Cartilage Tissue Engineering and Relevant Approaches for Future Development. *Tissue Eng Regen Med*, 2018. 15(6): p. 673-697.
4. Lee, K.Y. and D.J.J.C.r. Mooney, Hydrogels for tissue engineering. 2001. 101(7): p. 1869-1880.
5. Albuquerque, M., et al., Tissue-engineering-based strategies for regenerative endodontics. 2014. 93(12): p. 1222-1231.
6. Zhang, L. and I.R.J.I. Tizard, Activation of a mouse macrophage cell line by acemannan: the major carbohydrate fraction from Aloe vera gel. 1996. 35(2): p. 119-128.
7. Trinh, H.A., et al., Acemannan Induced Bone Regeneration in Lateral Sinus Augmentation Based on Cone Beam Computed Tomographic and Histopathological Evaluation. 2020. 2020.
8. Songsiripradubboon, S., et al., Stimulation of dentin regeneration by using acemannan in teeth with lipopolysaccharide-induced pulp inflammation. 2017. 43(7): p. 1097-1103.
9. Songsiripradubboon, S., et al., Clinical, radiographic, and histologic analysis of the effects of acemannan used in direct pulp capping of human primary teeth: short-term outcomes. 2016. 104(3): p. 329-337.
10. Vu, T.T., et al., Acemannan used as an implantable biomaterial for vital pulp therapy of immature permanent teeth induced continued root formation. 2020. 12(7): p. 644.
11. Huang, G.T., Pulp and dentin tissue engineering and regeneration: current progress. *Regen Med*, 2009. 4(5): p. 697-707.
12. Berman, L.H., L. Blanco, and S. Cohen, *A Clinical Guide to Dental Traumatology-E-Book*. 2006: Elsevier Health Sciences.

13. Huang, G.T., A paradigm shift in endodontic management of immature teeth: conservation of stem cells for regeneration. *J Dent*, 2008. 36(6): p. 379-86.
14. Sun, H.H., et al., Biological approaches toward dental pulp regeneration by tissue engineering. *J Tissue Eng Regen Med*, 2011. 5(4): p. e1-16.
15. Lin, L., et al., Clinical cell-based vs cell-free regenerative endodontics: Clarification of concept and term. *International Endodontic Journal*, 2021. 54(6).
16. Iwaya, S.I., M. Ikawa, and M. Kubota, Revascularization of an immature permanent tooth with apical periodontitis and sinus tract. *Dent Traumatol*, 2001. 17(4): p. 185-7.
17. Torabinejad, M. and H. Faras, A clinical and histological report of a tooth with an open apex treated with regenerative endodontics using platelet-rich plasma. *J Endod*, 2012. 38(6): p. 864-8.
18. Zizka, R. and J. Sedy, Paradigm Shift from Stem Cells to Cell-Free Regenerative Endodontic Procedures: A Critical Review. *Stem Cells Dev*, 2017. 26(3): p. 147-153.
19. Lovelace, T.W., et al., Evaluation of the delivery of mesenchymal stem cells into the root canal space of necrotic immature teeth after clinical regenerative endodontic procedure. *J Endod*, 2011. 37(2): p. 133-8.
20. Huang, G.T.-J., et al., Stem/progenitor cell-mediated de novo regeneration of dental pulp with newly deposited continuous layer of dentin in an in vivo model. *Tissue Engineering Part A*, 2010. 16(2): p. 605-615.
21. Manivasagam, G., et al., Dentistry: Restorative and Regenerative Approaches. *Encyclopedia of Biomedical Engineering*, 2019. 1(3): p. 332-347.
22. Zhang, W., et al., Osteo-/odontogenic differentiation of BMP2 and VEGF gene-co-transfected human stem cells from apical papilla. *Mol Med Rep*, 2016. 13(5): p. 3747-54.
23. Smith, A.J., et al., Dentine as a bioactive extracellular matrix. *Archives of Oral Biology*, 2012. 57(2): p. 109-121.
24. Piva, E., A.F. Silva, and J.E. Nor, Functionalized scaffolds to control dental pulp stem cell fate. *J Endod*, 2014. 40(4 Suppl): p. S33-40.
25. Galler, K.M., et al., Scaffolds for dental pulp tissue engineering. *Adv Dent Res*, 2011. 23(3): p. 333-9.

26. Rizk, H.M., M.S.M. Salah Al-Deen, and A.A. Emam, Comparative evaluation of Platelet Rich Plasma (PRP) versus Platelet Rich Fibrin (PRF) scaffolds in regenerative endodontic treatment of immature necrotic permanent maxillary central incisors: A double blinded randomized controlled trial. *Saudi Dent J*, 2020. 32(5): p. 224-231.
27. Petrino, J.A., et al., Challenges in regenerative endodontics: a case series. *J Endod*, 2010. 36(3): p. 536-41.
28. Jadhav, G.R., N. Shah, and A. Logani, Comparative outcome of revascularization in bilateral, non-vital, immature maxillary anterior teeth supplemented with or without platelet rich plasma: A case series. *Journal of conservative dentistry: JCD*, 2013. 16(6): p. 568.
29. Raddall, G., I. Mello, and B.M. Leung, Biomaterials and Scaffold Design Strategies for Regenerative Endodontic Therapy. *Front Bioeng Biotechnol*, 2019. 7: p. 317.
30. Miller, E.J. and R.K. Rhodes, [2] Preparation and characterization of the different types of collagen, in *Methods in enzymology*. 1982, Elsevier. p. 33-64.
31. Ward, A.G. and A. Courts, *Science and technology of gelatin*. 1977: Academic Press.
32. Hulmes, D., Collagen diversity, synthesis and assembly, in *Collagen*. 2008, Springer. p. 15-47.
33. Fraser, R.D., T.P. MacRae, and E. Suzuki, Chain conformation in the collagen molecule. *J Mol Biol*, 1979. 129(3): p. 463-81.
34. Piez, K.A., Molecular and aggregate structures of the collagens. *Extracellular matrix biochemistry*, 1984. 5.
35. van der Rest, M. and R. Garrone, Collagen family of proteins. *FASEB J*, 1991. 5(13): p. 2814-23.
36. Gelse, K., E. Pöschl, and T. Aigner, Collagens—structure, function, and biosynthesis. *Advanced drug delivery reviews*, 2003. 55(12): p. 1531-1546.
37. Lucas, P.A., et al., Ectopic induction of cartilage and bone by water-soluble proteins from bovine bone using a collagenous delivery vehicle. 1989. 23(S13): p. 23-39.
38. Yang, H., Z.J.J.o.c. Shu, and p. research, The extraction of collagen protein from pigskin. 2014. 6(2): p. 683-687.

39. Gorlov, I.F., et al., Collagen from porcine skin: a method of extraction and structural properties. *International Journal of Food Properties*, 2018. 21(1): p. 1031-1042.
40. Li, D., et al., Ultrasonic irradiation in the enzymatic extraction of collagen. *Ultrason Sonochem*, 2009. 16(5): p. 605-9.
41. Kim, H.K., et al., Effects of ultrasonic treatment on collagen extraction from skins of the sea bass *Lateolabrax japonicus*. *Fisheries Science*, 2012. 78(2): p. 485-490.
42. Kittiphattanabawon, P., et al., Isolation and characterization of collagen from the cartilages of brownbanded bamboo shark (*Chiloscyllium punctatum*) and blacktip shark (*Carcharhinus limbatus*). *Lwt-Food Science and Technology*, 2010. 43(5): p. 792-800.
43. Toldra, F., et al., Innovations in value-addition of edible meat by-products. *Meat Science*, 2012. 92(3): p. 290-296.
44. Saito, M., et al., Effect of collagen hydrolysates from salmon and trout skins on the lipid profile in rats. *J Agric Food Chem*, 2009. 57(21): p. 10477-82.
45. Kittiphattanabawon, P., et al., Characterisation of acid-soluble collagen from skin and bone of bigeye snapper (*Priacanthus tayenus*). *Food Chemistry*, 2005. 89(3): p. 363-372.
46. Schmidt, M.M., et al., Collagen extraction process. *International Food Research Journal*, 2016. 23(3): p. 913-922.
47. Friess, W.J.E.j.o.p. and biopharmaceutics, Collagen–biomaterial for drug delivery. 1998. 45(2): p. 113-136.
48. Capella-Monsonis, H., et al., An experimental toolbox for characterization of mammalian collagen type I in biological specimens. *Nature Protocols*, 2018. 13(3): p. 507-529.
49. Lynn, A.K., I.V. Yannas, and W. Bonfield, Antigenicity and immunogenicity of collagen. *J Biomed Mater Res B Appl Biomater*, 2004. 71(2): p. 343-54.
50. Zhang, D., et al., The development of collagen based composite scaffolds for bone regeneration. *Bioact Mater*, 2018. 3(1): p. 129-138.
51. Ebenezer, V., R.J.B. Balakrishnan, and P. Journal, Impact of Hemostatic Agents in Oral Surgery. 2015. 7(1): p. 215-219.

52. Bubalo, M., et al., The use of collagen membranes in guided tissue regeneration. *Vojnosanitetski Pregled*, 2017. 74(8): p. 767-772.
53. Reddy, G.S., et al., Membrane Assisted Palatal Fistula Closure in a Cleft Palate Patient: A Novel Technique. *J Clin Diagn Res*, 2016. 10(3): p. ZD22-4.
54. Li, X., et al., Guided bone regeneration using collagen membranes for sinus augmentation. *British Journal of Oral & Maxillofacial Surgery*, 2012. 50(1): p. 69-73.
55. Block, M.S. and B. Kelley, Horizontal Posterior Ridge Augmentation: The Use of a Collagen Membrane Over a Bovine Particulate Graft: Technique Note. *Journal of Oral and Maxillofacial Surgery*, 2013. 71(9): p. 1513-1519.
56. Birkenfeld, F., et al., Mechanical properties of collagen membranes modified with pores—are they still sufficient for orbital floor reconstruction? 2015. 53(10): p. 957-962.
57. Zhang, W., et al., The performance of human dental pulp stem cells on different three-dimensional scaffold materials. *Biomaterials*, 2006. 27(33): p. 5658-68.
58. Sumita, Y., et al., Performance of collagen sponge as a 3-D scaffold for tooth-tissue engineering. *Biomaterials*, 2006. 27(17): p. 3238-3248.
59. Zhang, L., et al., Review scaffold design and stem cells for tooth regeneration. 2013. 49(1): p. 14-26.
60. Prescott, R.S., et al., In vivo generation of dental pulp-like tissue by using dental pulp stem cells, a collagen scaffold, and dentin matrix protein 1 after subcutaneous transplantation in mice. 2008. 34(4): p. 421-426.
61. Jiang, X., H. Liu, and C. Peng, Clinical and Radiographic Assessment of the Efficacy of a Collagen Membrane in Regenerative Endodontics: A Randomized, Controlled Clinical Trial. *J Endod*, 2017. 43(9): p. 1465-1471.
62. Lee, C.H., A. Singla, and Y. Lee, Biomedical applications of collagen. *Int J Pharm*, 2001. 221(1-2): p. 1-22.
63. JoséFonseca, M., M.A. Alsina, and F.J.B.e.B.A.-B. Reig, Coating liposomes with collagen (Mr 50 000) increases uptake into liver. 1996. 1279(2): p. 259-265.
64. Kaufman, H.E., et al., Collagen-based drug delivery and artificial tears. *J Ocul Pharmacol*, 1994. 10(1): p. 17-27.

65. Suzuki, S., et al., Long-term follow-up study of artificial dermis composed of outer silicone layer and inner collagen sponge. 2000. 53(8): p. 659-666.
66. Nakashima, M., Induction of dentine in amputated pulp of dogs by recombinant human bone morphogenetic proteins-2 and -4 with collagen matrix. Arch Oral Biol, 1994. 39(12): p. 1085-9.
67. Nakashima, M. and K. Iohara, Regeneration of dental pulp by stem cells. Adv Dent Res, 2011. 23(3): p. 313-9.
68. Murakami, M., et al., The use of granulocyte-colony stimulating factor induced mobilization for isolation of dental pulp stem cells with high regenerative potential. Biomaterials, 2013. 34(36): p. 9036-9047.
69. Kwon, Y.S., et al., Behaviour of human dental pulp cells cultured in a collagen hydrogel scaffold cross-linked with cinnamaldehyde. Int Endod J, 2017. 50(1): p. 58-66.
70. Chandrasekaran, K.J.E.D.S., Aloe vera-A Herbal Panacea for Periodontal Disease? 2018. 17: p. 1749-1758.
71. Sajjad, A. and S.J.J.o.D.S. Subhani Sajjad, Aloe vera: An ancient herb for modern dentistry—A literature review. 2014. 2014.
72. Sierra-García, G.D., et al., Acemannan, an extracted polysaccharide from Aloe vera: A literature review. 2014. 9(8): p. 1934578X1400900836.
73. Liu, C., et al., Extraction, Purification, Structural Characteristics, Biological Activities and Pharmacological Applications of Acemannan, a Polysaccharide from Aloe vera: A Review. Molecules, 2019. 24(8): p. 1554.
74. Chokboribal, J., et al., Deacetylation affects the physical properties and bioactivity of acemannan, an extracted polysaccharide from Aloe vera. Carbohydr Polym, 2015. 133: p. 556-66.
75. Thunyakitpisal, P., et al., Acemannan increases NF- κ B/DNA binding and IL-6/-8 expression by selectively binding Toll-like receptor-5 in human gingival fibroblasts. 2017. 161: p. 149-157.
76. Lee, J.K., et al., Acemannan purified from Aloe vera induces phenotypic and functional maturation of immature dendritic cells. Int Immunopharmacol, 2001. 1(7): p. 1275-84.

77. Boonyagul, S., et al., Effect of acemannan, an extracted polysaccharide from Aloe vera, on BMSCs proliferation, differentiation, extracellular matrix synthesis, mineralization, and bone formation in a tooth extraction model. *Odontology*, 2014. 102(2): p. 310-7.
78. Shi, X.D., et al., Structural and conformational characterization of linear O-acetyl-glucomannan purified from gel of Aloe barbadensis Miller. *Int J Biol Macromol*, 2018. 120(Pt B): p. 2373-2380.
79. Kumar, S. and R. Kumar, Role of acemannan O-acetyl group in murine radioprotection. *Carbohydr Polym*, 2019. 207: p. 460-470.
80. Chow, J.T.N., et al., Chemical characterization of the immunomodulating polysaccharide of Aloe vera L. *Carbohydrate Research*, 2005. 340(6): p. 1131-1142.
81. Kumar, S. and A.B. Tiku, Immunomodulatory potential of acemannan (polysaccharide from Aloe vera) against radiation induced mortality in Swiss albino mice. *Food and Agricultural Immunology*, 2016. 27(1): p. 72-86.
82. Quezada, M.P., et al., Acemannan and Fructans from Aloe vera (Aloe barbadensis Miller) Plants as Novel Prebiotics. *Journal of Agricultural and Food Chemistry*, 2017. 65(46): p. 10029-10039.
83. Im, S.A., et al., Identification of optimal molecular size of modified Aloe polysaccharides with maximum immunomodulatory activity. *Int Immunopharmacol*, 2005. 5(2): p. 271-9.
84. Salah, F., et al., Effect of the deacetylation degree on the antibacterial and antibiofilm activity of acemannan from Aloe vera. *Industrial Crops and Products*, 2017. 103: p. 13-18.
85. Best, T., et al., Acute effects of a dietary non-starch polysaccharide supplement on cognitive performance in healthy middle-aged adults. *Nutr Neurosci*, 2015. 18(2): p. 76-86.
86. Kim, H.S. and B.M. Lee, Inhibition of benzo[a]pyrene-DNA adduct formation by Aloe barbadensis Miller. *Carcinogenesis*, 1997. 18(4): p. 771-6.
87. Bhalang, K., P. Thunyakitpisal, and N. Rungsirisatean, Acemannan, a Polysaccharide Extracted from Aloe vera, Is Effective in the Treatment of Oral

Aphthous Ulceration. *Journal of Alternative and Complementary Medicine*, 2013. 19(5): p. 429-434.

88. Kaya, G.S., et al., Comparison of alvogyl, SaliCept patch, and low-level laser therapy in the management of alveolar osteitis. *J Oral Maxillofac Surg*, 2011. 69(6): p. 1571-7.

89. Jettanacheawchankit, S., et al., Acemannan stimulates gingival fibroblast proliferation; expressions of keratinocyte growth factor-1, vascular endothelial growth factor, and type I collagen; and wound healing. 2009. 109(4): p. 525-531.

90. Shi, X.-D., et al., Polysaccharide from leaf skin of *Aloe barbadensis* Miller: Part I. Extraction, fractionation, physicochemical properties and structural characterization. 2017. 73: p. 176-183.

91. Chantarawatit, P., et al., Acemannan sponges stimulate alveolar bone, cementum and periodontal ligament regeneration in a canine class II furcation defect model. 2014. 49(2): p. 164-178.

92. Jittapiromsak, N., et al., Acemannan, an extracted product from *Aloe vera*, stimulates dental pulp cell proliferation, differentiation, mineralization, and dentin formation. 2010. 16(6): p. 1997-2006.

93. Jittapiromsak, N., et al., Acemannan, an extracted product from *Aloe vera*, stimulates dental pulp cell proliferation, differentiation, mineralization, and dentin formation. *Tissue Eng Part A*, 2010. 16(6): p. 1997-2006.

94. Songsiripradubboon, S., et al., Clinical, radiographic, and histologic analysis of the effects of acemannan used in direct pulp capping of human primary teeth: short-term outcomes. *Odontology*, 2016. 104(3): p. 329-337.

95. Vu, T.T., et al., Acemannan Used as an Implantable Biomaterial for Vital Pulp Therapy of Immature Permanent Teeth Induced Continued Root Formation. *Pharmaceutics*, 2020. 12(7): p. 644.

96. Nalinanon, S., et al., Use of pepsin for collagen extraction from the skin of bigeye snapper (*Priacanthus tayenus*). *Food Chemistry*, 2007. 104(2): p. 593-601.

97. Neuman, R.E. and M.A. Logan, The determination of hydroxyproline. *J Biol Chem*, 1950. 184(1): p. 299-306.

98. Cissell, D.D., et al., A Modified Hydroxyproline Assay Based on Hydrochloric Acid in Ehrlich's Solution Accurately Measures Tissue Collagen Content. *Tissue Eng Part C Methods*, 2017. 23(4): p. 243-250.
99. Smith, B., SDS polyacrylamide gel electrophoresis of proteins, in *Proteins*. 1984, Springer. p. 41-55.
100. Laemmli, U.K., Cleavage of structural proteins during the assembly of the head of bacteriophage T4. *Nature*, 1970. 227(5259): p. 680-5.
101. Timmons, T.M. and B.S. Dunbar, [51] Protein blotting and immunodetection, in *Methods in enzymology*. 1990, Elsevier. p. 679-688.
102. Gopal, R., et al., Applications of circular dichroism for structural analysis of gelatin and antimicrobial peptides. *Int J Mol Sci*, 2012. 13(3): p. 3229-44.
103. Ni, Y., et al., Isolation and characterization of structural components of Aloe vera L. leaf pulp. *Int Immunopharmacol*, 2004. 4(14): p. 1745-55.
104. Chokboribal, J., et al., Deacetylation affects the physical properties and bioactivity of acemannan, an extracted polysaccharide from Aloe vera. 2015. 133: p. 556-566.
105. Songsiripradubboon, S., et al., Stimulation of Dentin Regeneration by Using Acemannan in Teeth with Lipopolysaccharide-induced Pulp Inflammation. *Journal of Endodontics*, 2017. 43(7): p. 1097-1103.
106. Chokboribal, J., et al., Deacetylation affects the physical properties and bioactivity of acemannan, an extracted polysaccharide from Aloe vera. *Carbohydrate Polymers*, 2015. 133: p. 556-566.
107. Stewart, J.J.P., Optimization of parameters for semiempirical methods I. *Method. Journal of Computational Chemistry*, 1989. 10(2): p. 209-220.
108. M.J. Frisch, e.a., *Gaussian 09*. 2014, Gaussian, Inc.: Wallingford, CT.
109. Bella, J., B. Brodsky, and H.M. Berman, Hydration structure of a collagen peptide. *Structure*, 1995. 3(9): p. 893-906.
110. Pettersen, E.F., et al., UCSF Chimera - A visualization system for exploratory research and analysis. *Journal of Computational Chemistry*, 2004. 25(13): p. 1605-1612.

111. Eberhardt, J., et al., AutoDock Vina 1.2.0: New Docking Methods, Expanded Force Field, and Python Bindings. *Journal of Chemical Information and Modeling*, 2021. 61(8): p. 3891-3898.
112. Trott, O. and A.J. Olson, Software news and update AutoDock Vina: Improving the speed and accuracy of docking with a new scoring function, efficient optimization, and multithreading. *Journal of Computational Chemistry*, 2010. 31(2): p. 455-461.
113. Jeevithan, E., et al., Isolation, purification and characterization of pepsin soluble collagen isolated from silvertip shark (*Carcharhinus albimarginatus*) skeletal and head bone. 2014. 49(10): p. 1767-1777.
114. Terzi, A., et al., Effects of processing on structural, mechanical and biological properties of collagen-based substrates for regenerative medicine. 2018. 8(1): p. 1-13.
115. Boonyagul, S., et al., Effect of acemannan, an extracted polysaccharide from *Aloe vera*, on BMSCs proliferation, differentiation, extracellular matrix synthesis, mineralization, and bone formation in a tooth extraction model. 2014. 102(2): p. 310-317.
116. Martins, V.G., J.A.V. Costa, and C.J.Q.N. Prentice-Hernández, Hidrolizado protéico de pescado obtido por vias química e enzimática a partir de corvina (*Micropogonias furnieri*). 2009. 32: p. 61-66.
117. Kittiphattanabawon, P., et al., Isolation and characterisation of collagen from the skin of brownbanded bamboo shark (*Chiloscyllium punctatum*). 2010. 119(4): p. 1519-1526.
118. Dowling, D.P., et al., Effect of surface wettability and topography on the adhesion of osteosarcoma cells on plasma-modified polystyrene. 2011. 26(3): p. 327-347.
119. Elliott, J.T., et al., The effect of surface chemistry on the formation of thin films of native fibrillar collagen. 2007. 28(4): p. 576-585.
120. Campos, D.M., G.A. Soares, and K.J.B. Anselme, Role of culture conditions on in vitro transformation and cellular colonization of biomimetic HA-Col scaffolds. 2013. 3(2): p. e24922.

121. JITTAPIROMSAK, N., et al., Effect of acemannan on BMP-2 expression in primary pulpal fibroblasts and periodontal fibroblasts, in vitro study. 2007. 4(3): p. 149-154.
122. Dou, D., et al., Sequential releasing of VEGF and BMP-2 in hydroxyapatite collagen scaffolds for bone tissue engineering: Design and characterization. 2019. 123: p. 622-628.
123. Huang, B., et al., Distribution of SIBLING proteins in the organic and inorganic phases of rat dentin and bone. 2008. 116(2): p. 104-112.
124. Park, J.-C., et al., Influence of TGF- β 1 on the expression of BSP, DSP, TGF- β 1 receptor I and Smad proteins during reparative dentinogenesis. 2008.
125. Pechanika Lardungdee, D., D. Pornpun Asvanit, and D. Pasutha Thunyakitpisal, Effect of acemannan on the dentinsialophosphoprotein and dentin matrix protein 1 mRNA expressions in primary human pulpal cells.
126. Kognole, A.A. and C.M.J.J.o.B.C. Payne, Inhibition of mammalian glycoprotein YKL-40: identification of the physiological ligand. 2017. 292(7): p. 2624-2636.
127. Jayakumar, G.C., et al., Studies on the physico-chemical characteristics of collagen-pectin composites. 2014. 4(109): p. 63840-63849.
128. Kyriakides, T., Chapter 5-Molecular Events at Tissue-Biomaterial Interface. in (ed. Badylak, SFBT-HR to B.) 81-116. 2015, Academic Press.
129. Xing, W., et al., Acemannan accelerates cell proliferation and skin wound healing through AKT/mTOR signaling pathway. 2015. 79(2): p. 101-109.
130. Sularsih, S., et al., In Silico Analysis of Glycosaminoglycan-Acemannan as a Scaffold Material on Alveolar Bone Healing. 2022.
131. Kresnoadi, U., et al., TLR2 signaling pathway in alveolar bone osteogenesis induced by aloe vera and xenograft (XCB). 2017. 28: p. 281-286.
132. Zhou, Q., et al., The use of TLR2 modified BMSCs for enhanced bone regeneration in the inflammatory micro-environment. 2019. 47(1): p. 3329-3337.

VITA

NAME Aye Aye Thant

DATE OF BIRTH 31 March 1985

PLACE OF BIRTH Yangon, Myanmar

INSTITUTIONS ATTENDED B.D.S (University of dental medicine, Yangon, Myanmar)
M.D.Sc (Conservative Dentistry) (University of dental medicine, Yangon, Myanmar)

HOME ADDRESS no. 39, Bo Zin Yaw street, 30th block, North Dagon Myothit, Yangon, Myanmar.



จุฬาลงกรณ์มหาวิทยาลัย
CHULALONGKORN UNIVERSITY